



Degradation of dibutyl phthalate from synthetic and real wastewater using ultrasound/hydrogen peroxide system

Majid Nozari^{a,b}, Mohammad Malakootian^{a,b,*}, Neamatalah Jaafarzadeh Haghighi Fard^{c,d}, Hadi Mahmoudi-Moghaddam^{a,b}

^aEnvironmental Health Engineering Research Center, Kerman University of Medical Sciences, Kerman, Iran, Postal Code: 7616913555, Tel.: 98-9131401536; emails: m.malakootian@yahoo.com/m_malakootian@kmu.ac.ir (M. Malakootian), nozari.m@kmu.ac.ir (M. Nozari), h.mahmoudi@kmu.ac.ir (H. Mahmoudi-Moghaddam)

^bDepartment of Environmental Health Engineering, Faculty of Public Health, Kerman University of Medical Sciences, Kerman, Iran

^cEnvironmental Technologies Research Center, Ahvaz Jundishapur University of Medical Sciences, Ahvaz, Iran, email: Jaafarzadeh-n@ajums.ac.ir/n.jaafarzade@gmail.com (N.J.H. Fard)

^dDepartment of Environmental Health Engineering, School of Health, Ahvaz Jundishapur University of Medical Sciences, Ahvaz, Iran

Received 7 November 2022; Accepted 5 February 2023

ABSTRACT

Dibutyl phthalate (DBP) is the most prevalent phthalate ester found in different environmental samples. DBP is considered a hazardous substance for the environment. The degradation of DBP using an ultrasonic/hydrogen peroxide (US/H₂O₂) system has been studied in this study. Designing the experiments and determining optimal conditions were accomplished using the response surface methodology. The effects of the solution pH, H₂O₂ and DBP concentrations, and reaction time on the DBP degradation were studied. Kinetics and thermodynamics models, mineralization of DBP, production of intermediates, and biotoxicity analysis were also investigated. Finally, the real industrial wastewater treatment was tested using the US/H₂O₂ system. The result of the kinetic model showed that the removal kinetic of DBP can be described by the first-order model ($R^2 = 0.99$). The positive value of ΔH° (0.3 kJ/mol) and negative values of ΔG° indicated that the removal process of DBP by US/H₂O₂ was endothermic and spontaneous. In addition, a positive value of the ΔS° (1.054 J/mol·K) showed a high degree of disorder in the transition state compared to the ground state. A relatively high degree of mineralization and improvement in biodegradability occurred. A biotoxicity test was performed using the wheat grains, and an increase in the values of germination percentage GP (%), germination speed (GS), and germination index (GI) parameters of wheat grains was observed with the increase in effluent dilution. The EC₅₀ had an increasing trend at first (24 to 48 h) and then decreased (48 to 96 h). The average removal efficiency of DBP from industrial wastewater by the US/H₂O₂ system was 70.53%. This finding showed a relatively good potential US/H₂O₂ system to degrade an aqueous medium polluted with DBP.

Keywords: Dibutyl phthalate; Ultrasonic; Hydrogen peroxide; Industrial wastewater

1. Introduction

Phthalate esters (PAEs) have been applied in various industrial applications to improve plastics' processing and

moulding properties [1,2]. The US Environmental Protection Agency (USEPA) classified six types of PAEs as priority-controlled contamination compounds, namely di-*n*-butyl phthalate (DBP), butyl benzyl phthalate (BBP), di-*n*-octyl

* Corresponding author.

phthalate (DnOP), diethyl phthalate (DEP), dimethyl phthalate (DMP), and di(2-ethylhexyl)phthalate (DEHP) [1]. There is a high probability of DBP being detected in water, soil, and sediment when it comes to PAEs [3,4]. DBP concentrations exceeding 0.003 mg/L are not permissible under Chinese Surface Water Quality Standards [5,6]. The average concentration of the DBP in the effluent collected from the five wastewater treatment plants (WTPs) in Saudi Arabia was reported at 0.748 µg/L [7]. DBP is classified as a teratogen under California's Proposition 65 list [7]. The Consumer Product Safety Improvement Act (CPSIA) forbids the use of DBP in toys and childcare products in concentrations of more than 1,000 mg/L [8]. DBP is a relatively stable compound in the natural environment with a half-life of 5–20 y [8].

Plasticizers were not anticipated to become one of the most prevalent hazards to human health and the environment during their application's initial phase [1]. PAEs may disrupt the endocrine glands and have adverse effects on reproduction. In addition, PAEs can migrate over time as the environment changes [9–13]. Consequently, PAEs can be found in indoor food [14], dust [15], water [16], soil [17] and air [18].

Water is recognized as a vital component of life on earth [19]. Water contamination is a huge global environmental issue since it poses a substantial global threat to living species and the overall ecosystem's equilibrium [20–23]. Contaminants in the environment can be attributed to both natural and artificial sources [24,25]. A wide range of harmful contaminants from numerous chemical industries and daily activities are discharged into waterbodies [26,27]. Heavy metals, salts, pesticides, dyes, radioactive materials, and organic pollutants are examples of anthropogenic contaminants that are often released during various industrial processes [28–30]. Due to the increase in water demand worldwide every year, wastewater treatment is necessary to restore freshwater for human and agricultural use [31–33]. Based on mentioned points, industrial wastewater must be treated effectively before being released into the environment.

To remove PAEs from aqueous solutions, a variety of methods have been used, such as microbial degradation [34], photochemical degradation [35], and membranes [36]. Compared with other refractory organics, DBP is more easily biodegradable, and biodegradation is the most common and inexpensive method among all treatment methods. Nevertheless, the biodegradation method is time-consuming. Also, other procedures usually are ineffective, expensive and do not offer complete removal. Among the promising physicochemical methods are advanced oxidation processes (AOPs) as a combined method based on chemical solutions that are mainly applied, including AOPs. In AOPs, a reaction with a hydroxyl radical ($\cdot\text{OH}$) generated in the reaction medium is encouraged through the application of hydrogen peroxide (H_2O_2), ozone (O_3), an ultrasonic field, UV radiation and catalysts such as Fe^{2+} or TiO_2 [36]. Therefore, many studies have examined the possibility of treating PAEs in aqueous solutions using AOPs in previous decades [37–40].

AOPs technologies in wastewater treatment have advantages and disadvantages. These technologies provide benefits such as decreased sludge generation, the ability to degrade a wide variety of various types of contaminants in aquatic systems, the mineralization of most organic

compounds in these environments, and others. However, the AOPs technologies also have disadvantages, such as relatively high operating and maintenance costs, production of intermediate compounds, complex chemistry according to specific pollutants, etc [41,42].

Ultrasound (US) irradiation is an energetic source that can be used to create positive holes and free radicals. Over the past few years, the US has been successfully used for many pollutants in wastewater treatment [43]. Several factors can affect the US degradation of contaminants, such as temperature, the intensity of US waves, frequency, material volatility, viscosity, surfactants, dissolved gases, etc. The US procedure does not require chemicals, oxidizing agents, or accelerators, and there are no product waste streams. Other advantages of the ultrasonic method include the absence of any mutagenic and carcinogenic by-products, lack of odour and taste problems, no need to use and store dangerous chemicals, and requiring little space to install the units. The relatively slow rate of US degradation is a downside [44]. Wastewater treatment by ozonation is limited by the need for relatively high values of O_3 . Consequently, the cost of O_3 production for high-strength wastewater is high. Energy and electricity consumption in the ozonation system is high, and O_3 has high corrosive properties. O_3 can be dangerous in terms of being flammable. The ozonation system needs expert staff to set up and operate [45]. An ultraviolet (UV) system in a long-term application can cause skin burns and even cause cancer. Also, this system consumes a lot of electricity and needs constant care and washing of lamps. After some time, the UV lamps may burn out and must be replaced. A UV system is generally considered an expensive treatment method [45]. Therefore, combining H_2O_2 with US ($\text{US}/\text{H}_2\text{O}_2$) may be better than combining it with UV ($\text{UV}/\text{H}_2\text{O}_2$) and ozone ($\text{O}_3/\text{H}_2\text{O}_2$) systems.

Since decades ago, synthetic organic pollutants have been degraded using the ultrasonic/hydrogen peroxide ($\text{US}/\text{H}_2\text{O}_2$) system [46–49]. Numerous types of research have been conducted on related processes, some of which are analogous to our work. The innovation of this study is that it is more thorough than other studies; in other studies, the procedures are not carried out entirely and concurrently. In this work, US with H_2O_2 were investigated, and the roles of each were studied to assess their efficacy in DBP degradation. Furthermore, the toxicity of DBP solution was investigated in this study, which was not done in most previous investigations. Also, the effects of the solution pH, H_2O_2 and DBP concentrations, and reaction time on the DBP degradation were studied. In addition, the mineralization of DBP, intermediate compounds formed in the decomposition of DBP, and kinetics and thermodynamics models were investigated. Finally, the real industrial wastewater treatment containing DBP was tested using the $\text{US}/\text{H}_2\text{O}_2$ system.

2. Materials and methods

2.1. Chemicals

The materials employed in this research were of analytical grade. The following materials were provided from Sigma-Aldrich Company (Saint Louis, MO, USA): methanol (CH_3OH), hydrochloric acid (HCl), DBP ($\text{C}_6\text{H}_4(\text{CO}_2\text{C}_4\text{H}_9)_2$)

with purity > 98%, sodium hydroxide (NaOH), H₂O₂, and chloroform (CHCl₃).

2.2. Equipment, devices and software

The material was vibrated using a shaker (Shanghai, China THZ-98A). Sample pH was adjusted with HCl and NaOH solutions using a pH meter (Jenway Model 3505). A TOC analyzer (model Shimadzu VCHS/CSN, Japan) was used to determine the levels of total organic carbon (TOC). Analysis of chemical oxygen demand (COD) and five-day biochemical oxygen demand (BOD₅) was performed with C5220 and C5210 methods, respectively, provided in the standard water and wastewater testing methodologies [50]. An ultrasonic bath (P60H, Elma, Germany) was used to provide the required ultrasonic waves. The power and frequency of the ultrasonic device were 550 W and 60 Hz, respectively.

A gas chromatography (GC) system with a flame ionization detector (FID) was used to analyze and measure residual DBP levels. The model of this system was YL Instrument 6500GC, Korea. The system had a TRB-5 capillary column (30 m × 0.53 mm × 11.5 μm). Hydrogen gas (H₂) was used as a carrier gas with a flow rate of 1.5 mL/min. The initial temperature of the oven was 60°C, which was kept at this temperature for 1 min. After that, the temperature was increased from 60°C to 280°C at 20°C/min. In the end, it was maintained at 280°C for 6 min. The sample with a volume of 2 μL was injected with a 10 μL Hamilton syringe. The temperature of the detector was 295°C. Also, the temperature of the injector was 290°C [51]. The limits of detection (LOD) and quantitation (LOQ) determined for DBP by the GC-FID instrument were 200 μg/L (0.2 mg/L) and 660 μg/L (0.66 mg/L), respectively. Also, R² values of calibration curves were in the range of 0.995–0.998.

A gas chromatography-mass spectrophotometer (GC-MS) (with a DB-5 fused silica capillary column) attached to a Mass TRACE (Manchester, UK) was employed to identify intermediates in the removal of DBP using the US/H₂O₂ system. Helium gas with a flow rate of 1 mL/min was used as carrier gas. The sample with a volume of 1 μL was injected into the device. The initial temperature of the oven was 70°C, which was kept at this temperature for 1 min. After that, it reached 280°C at 10°C/min. In the end, it was maintained at 280°C for 7 min [52].

The H₂O₂ concentrations were measured using the iodometry method by adding aliquots from the reactor into the quartz cuvette of the spectrophotometer containing potassium iodide (KI, 0.1 M) and ammonium heptamolybdate ((NH₄)₆Mo₇O₂₄, 0.01 M) [53].

Design-Expert software (version 12) was used to design experiments, analyze and determine optimal conditions. Also, the chemical structure and molecular weight of the identified intermediate compound were determined by Chem Draw Ultra software (version 12). To calculate the EC₅₀ value of the effluent of each process, Probit statistical test was used using SPSS software (version 25).

2.3. Extraction method of DBP

We utilized the liquid-liquid extraction (LLE) method to extract DBP from samples [54]. In the first step, a 10 mL

test tube was filled with 5 mL of the sample. A 5 mL pipette was then used to transfer 1.5 mL of organic solvent (chloroform, CHCl₃) into the aquatic sample and vortexed for 2 min. The water and organic solvent sample were separated into phases using a separatory funnel. As a final step, 2 μL of the organic phase was drawn with a Hamilton syringe and injected into the GC-FID device [55]. In this extraction method, a 98% recovery was achieved. The extraction procedure was carried out twice to ensure.

2.4. Methodology for testing

The schematic of the reactor used in the study is shown in Fig. 1. Because the temperature in the ultrasonic water bath increases over time. Furthermore, a constant temperature (temperature setting) was needed in thermodynamic studies. Therefore, we used a circulate flow system to cool the water bath of the system (Fig. 1). All the degradation studies were carried out in a beaker (250 mL). Temperature and mixing speed factors were not part of the design parameters. Therefore, these two parameters were considered constant) the temperature of 25°C and stirring speed of 700 rpm(. The matrix for the 30 runs provided by the software, kinetics and thermodynamics studies, and the intermediate compound identification tests was synthetic wastewater (contaminated distilled water). Other tests were performed with real industrial wastewater. Eq. (1) was used to compute DBP degradation efficiency (%) [56]:

$$R(\%) = \frac{(C_0 - C_f)}{C_0} \times 100 \quad (1)$$

where *R* refers to the DBP degradation efficiency (%), *C*₀ refers to the DBP initial concentration in an aqueous solution (mg/L), and *C*_{*f*} refers to the DBP final concentration in an aqueous solution (mg/L).

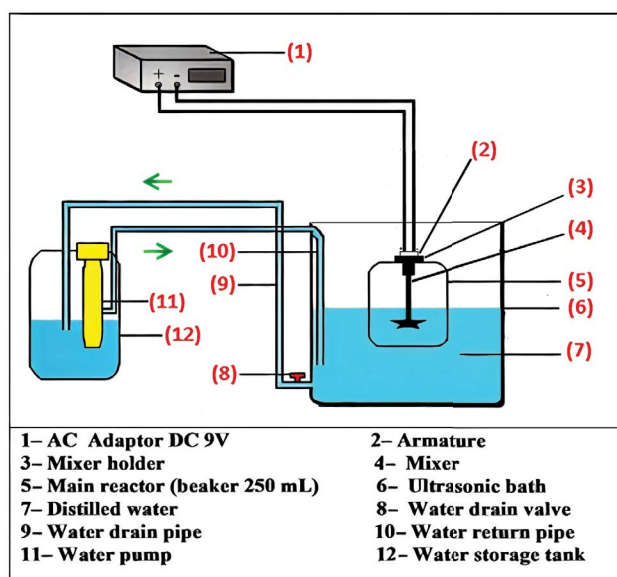


Fig. 1. Schematics of the reactor used in the study.

The effects of four variables of pH (3, 5, 7, 9 and 11), H₂O₂ concentration (0, 1, 1.5, 2 and 2.5 mmol/L), DBP concentration (6, 8, 10, 12 and 14 mg/L), and reaction time (15, 40, 65, 90 and 115 min) and their interaction on DBP removal efficiency were investigated. We selected a range of variables based on previous studies [56]. The design of the experiments was done with the central composite design (CCD) method by Design-Expert software. Based on the variables, 30 laboratory runs were provided by the software. Eq. (2) (quadratic polynomial response equation) was used to predict the optimal point:

$$Y = \beta_0 + \sum_{i=1}^k \beta_i X_i + \sum_{i=1}^k \beta_{ii} X_i^2 + \sum_{i=1}^{k-1} \sum_{j=i+1}^k \beta_{ij} X_i X_j \quad (2)$$

where Y is the DBP removal efficiency (%). β_0 , β_i , β_{ii} , β_{ij} and X_i are constant, linear, quadratic and interaction coefficients, respectively. X_i and K are coded independent variables and the number of input variables, respectively [56].

30 laboratory runs (with three repetitions) were performed to reach an optimal condition and obtain the actual removal efficiency. After performing the laboratory runs and obtaining the removal efficiency (%) for each run, the analysis was performed by Design-Expert software. Based on the analysis of variance (ANOVA) table, the compatibility of the proposed model (quadratic model) by the software with the experimental data was determined.

2.5. Degradation kinetics

A kinetic equation describes the transfer of molecules per unit of time or examines variables that affect the rate of a chemical reaction [57]. As part of this study, kinetic experiments were performed to determine factors that affect the reaction rate of DBP degradation by the US/H₂O₂ system to select an appropriate kinetic model. Also, by constructing a mathematical model of the decomposition reaction of DBP, its properties can be explained. A model of first-order kinetic was used for these purposes. All parameters were optimal in investigating the kinetics of DBP decomposition by the US/H₂O₂ system, and only the reaction time was considered variable (0–115 min). In this regard, a laboratory test was conducted to investigate the kinetics of the reaction. The first-order kinetics linear model and its half-life equation are shown in the supplementary file [58,59].

2.6. Degradation thermodynamics

Thermodynamic experiments evaluate the effect of temperature on DBP decomposition by the US/H₂O₂ system. In this regard, a laboratory test was conducted to investigate the thermodynamic behaviour of DBP degradation. The thermodynamic experiments also investigate the oxidation reaction's spontaneity, energy (exothermic or endothermic), and disorder state. Several thermodynamic parameters were investigated to determine how reaction temperature affects DBP removal. All parameters were optimal in investigating the thermodynamic behaviour of DBP degradation by the US/H₂O₂ system, and only the temperature was considered variable (303–343 K). According to the Arrhenius

equation, temperature influences the rate constant of chemical reactions [Eq. (3)]. A straight line with slope ($-E_a/R$) can be obtained when plotting $\ln(1/K)$ against $(1/T)$. The activation energy can be determined by the slope of this line [Eq. (4)]. According to Eqs. (5)–(7), thermodynamic parameters such as enthalpy changes (ΔH°), entropy changes (ΔS°), and Gibbs free energy (ΔG°) were calculated [60–62].

$$K = A e^{\frac{-E_a}{RT}} \quad (3)$$

$$\ln K = -\frac{E_a}{R} \left(\frac{1}{T} \right) + \ln A \quad (4)$$

$$\Delta G^\circ = \Delta H^\circ - T\Delta S^\circ \quad (5)$$

$$\Delta H^\circ = E_a - RT \quad (6)$$

$$\Delta S^\circ = R \left(\ln K_{\text{ref}} - \ln \left(\frac{K_b}{h_p} \right) - \ln T \right) \quad (7)$$

where A refers to the number of clashes resulting in a reaction or not (per second) with the appropriate orientation. K refers to the number of collisions that cause a reaction per second. T is the temperature (K). K_{ref} refers to the reaction rate constant at the reference temperature ($T_{\text{ref}} = 323$ K). R refers to the universal gas constant (8.314 J/mol·K). h_p refers to Planck's constant (6.626×10^{-34} J.s), and K_b refers to the Boltzmann constant (1.38×10^{-23} J/K) [59,63].

2.7. Biototoxicity analyses

Residual phthalates may damage plants and other creatures in wastewater treatment plant effluents. As a result, biototoxicity analyses on effluents generated by the US/H₂O₂ system are required. In this regard, two laboratory tests (one test for each sample) were performed in optimal conditions. Wheat (*Triticum*) seeds were used to assess the biototoxicity of effluent derived from the US/H₂O₂ system [64,65]. The inhibitory effects of DBP at concentrations of 5–20 mg/L on wheat seedlings were reported by Gao et al. [66]. According to this research [66], since the toxicity evaluation of raw wastewater containing DBP was investigated with wheat seeds, it was not tested in this study. To investigate the biototoxicity of effluent, the wheat seeds were sieved, and the almost uniform size and weight seeds were separated. After that, the seeds were steeped in distilled water for 24 h. 100 mL of effluent was collected from the operated reactor with real industrial wastewater under optimal conditions (samples #1 and 2). The collected effluent was divided into four dilutions (1, 1/2, 1/4, and 1/5). To be sure, each dilution was repeated once. Afterwards, 15 wheat seeds were planted in each Petri dish ($d = 10$ cm), and 15 mL of treated wastewater with suitable dilution was added to each. The Petri plates were stored at 27°C in the laboratory. Furthermore, a control sample was provided using distilled water. The number of germinated

and radicle seedlings was then counted after 24, 48, 72, and 96 h. The appearance of a root tip with a length of 1 mm was used as germinating criteria. Eventually, the germination percentage, speed, and index (GP (%), GS, and GI) factors were used to analyze the data. Eqs. (8)–(10) were used to calculate these factors [55,65]:

$$GP(\%) = \frac{N_i}{N} \times 100 \tag{8}$$

$$GS = \sum_{n=1}^i \left(\frac{N_i}{T_i} \right) \tag{9}$$

$$GI = \sum \frac{T_i N_i}{N} \tag{10}$$

In Eqs. (8)–(10) N_i is the number of germinated grains on the day i . N is the total number of grains. T_i refers to the number of days after implantation.

In addition, the average effective concentration (EC_{50} or the concentration of effluent that inhibits 50% of grain germination) was computed. The EC_{50} value was calculated with the Probit statistical test in SPSS₅₀ software (version 25).

3. Results and discussion

3.1. Experimental design using CCD-based response surface methodology

Table 1 presents an experimental design using CCD-based response surface methodology (RSM) for DBP removal by US/H₂O₂ system. The maximum efficiency of DBP removal (86.02%) was obtained in laboratory conditions

Table 1
Experimental design using CCD-based response surface methodology for DBP removal by US/H₂O₂ system (factor 1: pH (-), factor 2: DBP initial concentration (mg/L), factor 3: H₂O₂ initial concentration (mmol/L), factor 4: reaction time (min), and response: removal efficiency (%))

Run	Factor 1		Factor 2		Factor 3		Factor 4		Response		Standard deviation of actual removal efficiency (%)
	A: pH (-)		B: DBP initial concentration (mg/L)		C: H ₂ O ₂ initial concentration (mmol/L)		D: Reaction time (min)		Removal efficiency (%)		
									Predicted value	Actual value	
1	7	6			1.5		65		72.13	72.51	0.27
2	9	12			2		90		52.37	52.74	0.17
3	7	10			1.5		65		73.00	73.64	0.32
4	5	12			1		40		60.93	60.65	0.14
5	7	10			1.5		65		73.00	73.01	0.19
6	5	8			2		90		76.65	76.12	0.52
7	9	12			1		90		48.60	48.23	0.63
8	7	10			2.5		65		59.27	59.7	0.25
9	5	8			1		40		53.89	53.96	0.13
10	9	8			1		40		33.13	32.58	0.24
11	5	12			1		90		85.19	86.02	0.19
12	7	10			0.5		65		52.06	51.45	0.21
13	7	10			1.5		115		77.71	77.15	0.38
14	11	10			1.5		65		21.12	20.92	0.64
15	5	8			1		90		80.62	80.56	0.99
16	9	8			2		40		56.13	55.75	1.14
17	5	12			2		40		52.56	52.25	0.36
18	7	10			1.5		65		73.00	72.95	0.46
19	9	12			2		40		50.31	50.09	0.35
20	7	10			1.5		15		48.92	49.31	0.75
21	9	8			1		90		45.08	45.83	0.65
22	7	10			1.5		65		73.00	72.55	0.60
23	9	8			2		90		60.66	60.66	0.17
24	9	12			1		40		39.13	40.11	0.43
25	5	8			2		40		57.33	57.42	0.34
26	7	10			1.5		65		73.00	73	0.99
27	5	12			2		90		69.40	69.67	0.65
28	3	10			1.5		65		58.91	58.94	0.43
29	7	10			1.5		65		73.00	72.85	0.96
30	7	14			1.5		65		70.88	70.32	0.69

corresponding to run no. 11. The actual removal efficiency (%) had a standard deviation between 0.13% and 1.14%. Additionally, the removal efficiency values obtained for all runs in the laboratory were close to the removal efficiency values predicted by Design–Expert software (Table 1).

It has been proposed that a quadratic model describes the DBP degradation process by US/H₂O₂ system. Based on the R^2 value and p -value provided for the model, the difference between the predicted and adjusted R^2 value and the lack of fit p -value were concluded whether the quadratic model is suitable or not. The R^2 value of the model was 0.999, which was very close to 1. Moreover, the predicted R^2 value ($R^2 = 0.995$) was reasonably close to the adjusted R^2 value ($R^2 = 0.998$) because their difference was less than 0.2 (R^2 results are not presented in Table 2). Based on the ANOVA results presented in Table 2, a p -value of less than 0.05 for the model indicates that the model is statistically significant. A , B , C , D , AC , AD , BC , BD , CD , A^2 , B^2 , C^2 , and D^2 factors were significant in the model. Also, in this model, the lack of fit p -value was 0.07. Lack of fit p -value was greater than 0.05 and was not significant. A statistically insignificant lack of fit indicates the appropriateness of the model. Therefore, it can be concluded that the model provided by the software was suitable.

Furthermore, the extended investigation was performed using normality plots to check whether the proposed empirical model represents real responses best. Fig. S1a indicates the normal probability plot of the residuals since scattered points are near the predicted line, indicating that residual error follows the normal distribution trend [67,68]. Fig. S1b demonstrates the actual vs. predicted values graph of removal efficiency. The predicted points are close to the actual points. Therefore the proposed model is

adequate and has no violation of constant or independent variance [67,68].

For the quadratic model proposed by Design–Expert software for DBP removal by the US/H₂O₂ system, the following coded equation was presented [Eq. (11)]:

$$\begin{aligned} \text{Removal efficiency} = & +73 - 9.45(A) - 0.3125(A) \\ & + 1.8(C) + 7.2(D) - 0.2612(AB) \\ & + 4.89(AC) - 3.7(AD) - 2.95(BC) \\ & - 0.6187(BD) - 1.85(CD) - 8.25(A^2) \\ & - 0.3750(B^2) - 4.33(C^2) - 2.42(D^2) \end{aligned} \quad (11)$$

To predict the response for a given level of each factor, we can use Eq. (11) in terms of coded factors. Here, it is essential to specify the levels in the original units for each factor [69].

3.2. Investigating parameters affecting DBP degradation

The efficiency of DBP removal using the US/H₂O₂ system from an aqueous solution was increased by enhancing reaction time, as shown in Table 1 and Fig. 2a–f. Nevertheless, the degradation efficiency of DBP decreased as pH, DBP concentration, and H₂O₂ concentration increased.

3.2.1. Effect of pH on the DBP decomposition

The efficiency of the process is generally influenced by the pH of a solution [70]. Table 1 and Fig. 2a–c illustrates the effect of pH on the degradation efficiency of DBP by the US/

Table 2
Results of ANOVA provided by Design–Expert software for the removal of DBP by the US/H₂O₂ system

Source	Sum of squares	df	Mean square	F-value	p-value	
Model	6,480.24	14	462.87	1,220.26	<0.0001	Significant
A-pH	2,141.37	1	2,141.37	5,645.22	<0.0001	
B-Initial concentration of DBP	2.34	1	2.34	6.18	0.0252	
C-Initial concentration of H ₂ O ₂	77.98	1	77.98	205.57	<0.0001	
D-Reaction time	1,242.72	1	1,242.72	3,276.14	<0.0001	
AB	1.09	1	1.09	2.88	0.1104	
AC	382.40	1	382.40	1,008.10	<0.0001	
AD	218.74	1	218.74	576.67	<0.0001	
BC	139.71	1	139.71	368.32	<0.0001	
BD	6.13	1	6.13	16.15	0.0011	
CD	54.98	1	54.98	144.95	<0.0001	
A ²	1,865.16	1	1,865.16	4,917.06	<0.0001	
B ²	3.86	1	3.86	10.17	0.0061	
C ²	515.44	1	515.44	1,358.85	<0.0001	
D ²	160.80	1	160.80	423.91	<0.0001	
Residual	5.69	15	0.3793			
Lack of fit	5.05	10	0.5053	3.96	0.0708	Not significant
Pure error	0.6372	5	0.1274			
Cor. total	6,485.93	29				

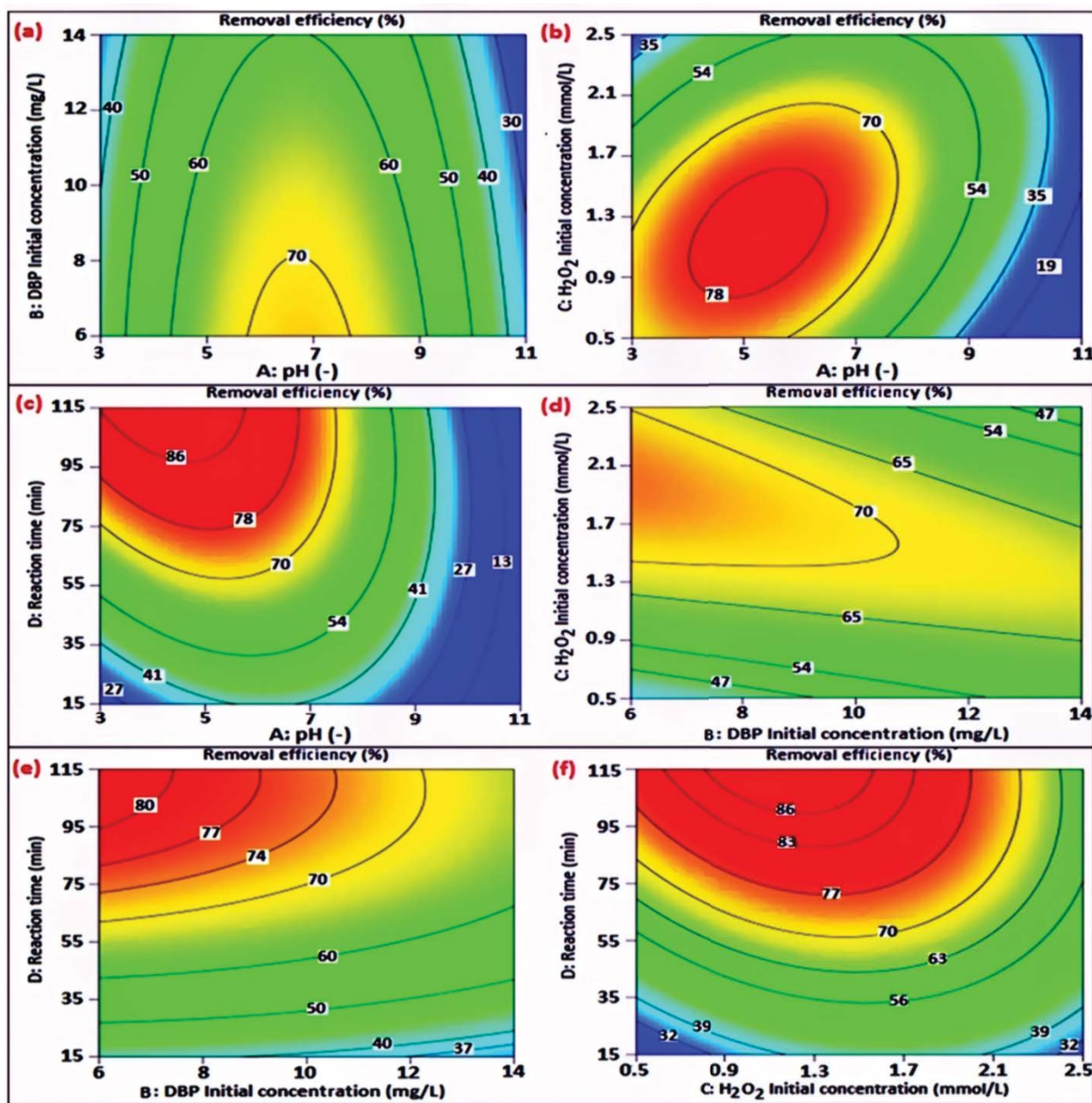


Fig. 2. The contour graphs and interactive effects of the considered factors on the DBP removal efficiency by US/H₂O₂ system; (a) pH vs. DBP initial concentration, (b) H₂O₂ initial concentration, and (c) reaction time, (d) DBP initial concentration vs. H₂O₂ initial concentration and (e) reaction time, (f) H₂O₂ initial concentration vs. reaction time.

H₂O₂ system in the pH range of 3–11. Based on the results, DBP removal efficiencies at pH 3, 5, 7, 9 and 11 were 58.94%, 52.25%–86.02%, 49.31%–77.15%, 32.58%–60.66% and 20.29%, respectively. The maximum efficiency of DBP removal was observed at pH = 5. The efficiency of DBP removal decreased as the pH of the solution increased, showing that the degradation of DBP was highly dependent on pH. DBP hydrophobic properties can be altered by a change in pH, which affects the ultrasonic degradation process [49]. The production of short-lived radicals created during intense cavitation events is commonly used for the sonochemical degradation of organic contaminants [36]. Although pH alone has

minimal influence on cavitation, the reaction of transient species escaping from bubbles can be affected by pH fluctuations [71]. The effect of pH during DBP degradation is probably due to the chemical structure and properties of DBP. Pollutant hydrophobicity is one of the most important factors for predicting the path of sonochemical reactions. Degradation of DBP will increase if hydrophobicity is favourable. DBP molecule is polar and has relatively high solubility (15 mg/L), low Henry's constant (0.27 Pa·m³/mol) and $K_{OW} = 5.4$. Therefore, DBP cannot penetrate the bubble and is mainly removed by $\cdot\text{OH}$ radicals in the solution volume or bubble surface. The degradation rate as a function

of pH is related to pK_a . The pK_a of DBP is about 2.9 [72]. Based on this, DBP is found mainly in molecular form in an acidic solution. Under these conditions, its hydrophobicity is favourable. It accumulates at the interface of the cavitation bubble, where there is a relatively high concentration of $\cdot\text{OH}$ radicals. As the pH increases, ionization occurs, and the hydrophobicity of DBP decreases. The decomposition of DBP occurs more in the solution bulk, where the concentration of $\cdot\text{OH}$ radicals is lower [72]. As a result, the decomposition rate of DBP decreases. Similarly, other researchers have reported that pH plays a significant role in the sonochemical degradation of organic compounds. For example, it has been shown that the removal efficiency of 4-nitrophenol decreases with increasing pH. This conclusion is explained by the fact that 4-nitrophenol may exist in the deprotonated form under acidic conditions (pK_a 4-nitrophenol = 7.08) and protonated (uncharged) form under basic conditions [71]. In addition, the degradation rate of DMP decreased with increasing pH in the 5–9 range [73]. According to Villaroel et al. [74] study, acetaminophen is more degraded in acidic solutions than in basic solutions. Therefore, pH was more likely influenced by the chemical structure and properties of the substance involved. A significant factor has certainly been revealed to be the hydrophobicity of the pollutant [74,75].

3.2.2. Effect of DBP concentration on the DBP decomposition

Table 1 and Fig. 2b, d and f demonstrate the effect of various concentrations (6–14 mg/L) on the degradation efficiency of DBP by US/ H_2O_2 . Based on the results, DBP removal efficiency was obtained to be 72.51%, 32.58%–80.56%, 20.92%–77.15%, 40.11%–86.02% and 70.32% in 6, 8, 10, 12 and 14 mg/L, respectively. We found that the maximum removal efficiency of DBP was obtained at an initial concentration of 12 mg/L. There was a gradual drop in the removal efficiency of DBP from 6 to 14 mg/L. The cause of this phenomenon can be explained as follows: since in this study, the frequency was constant (60 Hz), with increasing concentrations of DBP, sound waves did not reach the surface of all particles, and the production of $\cdot\text{OH}$ was decreased. Consequently, the degradation efficiency of DBP was decreased. Xu et al. [73] used high-frequency US process in their study to decompose DMP and observed a decrease in removal efficiency with increasing DMP concentration.

3.2.3. Effect of H_2O_2 concentration on the DBP decomposition

Table 1 and Fig. 2a, d, and e show the effects of different concentrations of H_2O_2 (0.5–2.5 mmol/L) on the removal efficiency of DBP using the US/ H_2O_2 system. Results showed that removal efficiency for DBP in 0.5, 1.0, 1.5, 2.0 and 2.5 mmol/L was 51.45%, 32.58%–86.02%, 20.92%–77.15%, 50.09%–76.12% and 59.7%, respectively. At an H_2O_2 concentration of 1 mmol/L, the maximum efficiency of DBP removal was achieved. The removal efficiency of H_2O_2 enhanced as the concentration increased from 0.5 to 1.5 mmol/L but then decreased again. According to several reports, when H_2O_2 molecules can scavenge decomposing organic pollutants, $\cdot\text{OH}$ that exists in the solution forms much fewer oxidative hydroperoxyl radicals ($\text{HO}_2\cdot$), which can be expressed as [76–78]:



In a study similar to the present one, researchers used a US process in the presence of H_2O_2 (concentrations of 0–1,000 mg/L) to decompose monochlorophenol ($\text{C}_6\text{H}_5\text{ClO}$); they found that excess H_2O_2 could react competitively with the $\cdot\text{OH}$ to form $\text{HO}_2\cdot$, especially in alkaline solution. They also found that $\text{HO}_2\cdot$ had much fewer oxidative effects and did not contribute to the degradation of $\text{C}_6\text{H}_5\text{ClO}$ [64]. Iordache et al. [79] used a US/ H_2O_2 system to decompose cyanide with different initial ratios $\text{CN}^-/\text{H}_2\text{O}_2$ (1/1, 1/3, 1/15 and 1/30 (g/g)); their results showed that with a decrease in the initial H_2O_2 amount, the time needed to complete cyanide degradation enhanced from 40 min at $\text{CN}^-/\text{H}_2\text{O}_2$:1/30 ratio to 115 min at $\text{CN}^-/\text{H}_2\text{O}_2$: 1/1 ratio. Therefore, it can be said that adding H_2O_2 to the US process can improve the removal of pollutants.

3.2.4. Effect of reaction time on the DBP decomposition

As shown in Table 1 and Fig. 2c, e, and f, a set of experiments was conducted to determine the effect of reaction time (15–115 min) on DBP removal by the US/ H_2O_2 system. Based on the results, DBP removal efficiency was obtained to be 49.31%, 32.58%–60.65%, 20.92%–73.64%, 45.83%–86.02% and 77.15% at 15, 40, 65, 90 and 115 min, respectively. The maximum removal efficiency was achieved after 90 min of reaction time. The removal efficiency of DBP increased as the reaction time increased. As the reaction time rose, the cavitation bubbles and their implosive energy increased, increasing the amount of $\cdot\text{OH}$ generated [80]. Xu et al. [80] used a US/ H_2O_2 system to decompose DMP. They found that the decomposition efficiency increased when the reaction time was increased from 0 to 300 min. Researchers used the ultrasonic method for removing cyanide [79], carbofuran [81], and pentachlorophenol [82]. Their results were similar to those in our studies.

3.3. Degradation of kinetic

We used the first-order kinetic model to investigate the kinetic of DBP removal by the US/ H_2O_2 system (Fig. 3). The result of the kinetic model showed that the removal kinetic of DBP can be described by the first-order model (K_1 (min^{-1}) = 0.009, $R^2 = 0.99$); this implies that the DBP concentration controls the DBP degradation rate by the US/ H_2O_2 system. Igwegbe et al. [83] studied the removal of ciprofloxacin from an aqueous solution using sonochemical, sono-nano-chemical and sono-nano-chemical/persulfate processes and reported that the kinetic data fitted well with the pseudo-first-order kinetic model. Also, Yegane Badi et al. [84] reported that the rate of reaction for catechol degradation in the US/ $\text{TiO}_2/\text{H}_2\text{O}_2$ process followed first-order kinetics. Similarly, half-life was also calculated using the half-life equation related to first-order kinetic. It was ascertained that the half-life value calculated through the first-order kinetic equation was closely related to the experimental values (45.21 min).

3.4. Degradation thermodynamics

From the slope of the Arrhenius plot in Fig. 4a, we calculated the E_a of the US/ H_2O_2 system to be 27.24 kJ/mol. The low value suggests that the oxidative reaction proceeds with a low energy barrier. Also, the sensitivity of reactions with less E_a is lower to temperature. In Fig. 4b, we found some other thermodynamic parameters like ΔH° and ΔS° from the Eyring–Polanyi plot. A positive value of the ΔH° (0.3 kJ/mol) indicated that the oxidative reaction was endothermic. Also, a positive value of the ΔS° (1.054 J/mol·K), implying that the transition state was highly disordered relative to the ground state (Table 3) [85]. As a result, the oxidative degradation reaction progressed quickly, which was desirable. Based on the values of the ΔH° and ΔS° at different temperatures, the ΔG° was calculated as a driving force of the oxidation reaction. The values were found to be -0.61, -0.94, -2.31, -2.89 and -4.39 kJ/mol at temperatures of 303, 313, 323, 333 and 343 K (Table 3). The negative values of ΔG° imply that the chemical reaction using the US/ H_2O_2 system to degrade DBP is spontaneous and that this spontaneity increases with temperature [85].

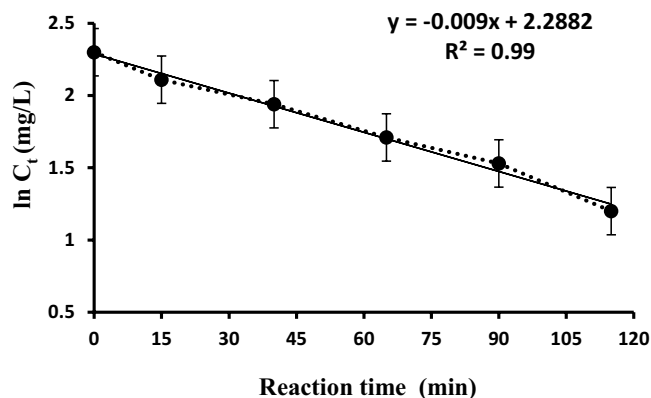


Fig. 3. Investigating first-order kinetic model for DBP removal by US/ H_2O_2 system (pH = 7, the concentration of H_2O_2 : 1.5 mmol/L, concentration of DBP: 10 mg/L, and reaction time: 0–115 min).

3.5. A proposed mechanism for removal of DBP by US/ H_2O_2 system

Decomposition of DBP in the US/ H_2O_2 system is done by $\cdot OH$ radicals that exist at the interface between the cavitation bubble and the aqueous phase. The probability of its decomposition by thermal pyrolysis in the bubble is very low. This possibility is supported by the hydrophobic nature and low volatility of DBP. Also, Xu et al. [73] used the US/ H_2O_2 system to remove dimethyl phthalate. Researchers added methanol as a hydroxyl radical scavenger to the system. They concluded that no elimination was observed after 115 min. As a result, DBP is degraded by $\cdot OH$ radicals as described by the following equation [73]:

$$\frac{d[\text{DBP}]}{dt} = -K_{\text{DBP}}[\cdot\text{OH}] \quad (12)$$

In the kinetic findings, K_{DBP} is achieved as first-order with a value of 0.009 min^{-1} . The present study used an ultrasonic bath with a fixed frequency (60 Hz). Therefore, it can be assumed that the production rate of $\cdot OH$ radicals and their concentration are constant during the ultrasound. In other words, the production of $\cdot OH$ radicals equals their consumption. The reactions that occur due to ultrasonic radiation in water are summarized below (R3–R13). During ultrasound

Table 3

Calculated thermodynamic parameters of the removal of DBP using the US/ H_2O_2 process (pH = 7, the concentration of H_2O_2 : 1.5 mmol/L, concentration of DBP: 10 mg/L, reaction time: 65 min, and different temperatures: 303–343 K)

T (K)	ΔH° (kJ/mol)	ΔS° (J/mol·K)	ΔG° (kJ/mol)
303			-0.61
313			-0.94
323	0.3	1.054	-2.31
333			-2.89
343			-4.39

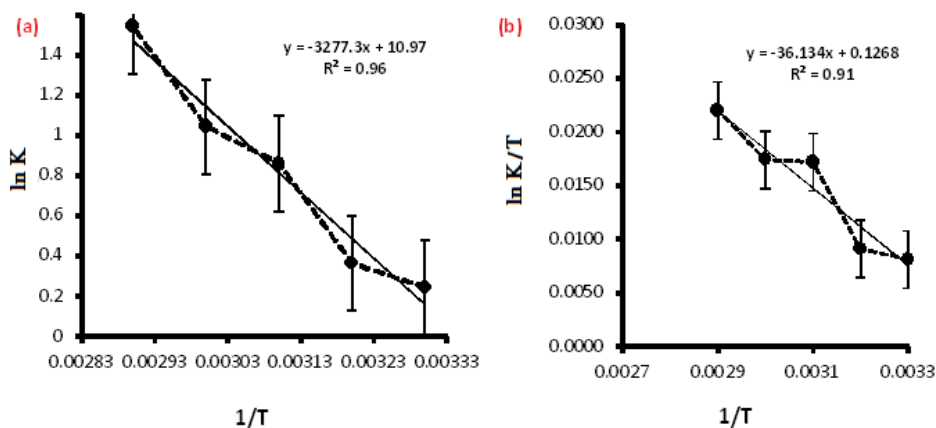


Fig. 4. Plots of (a) $\ln K$ vs. $1/T$ and (b) $\ln(K/T)$ vs. $1/T$ for the removal of DBP (pH = 7, the concentration of H_2O_2 : 1.5 mmol/L, concentration of DBP: 10 mg/L, reaction time: 65 min, and different temperatures: 303–343 K).

irradiation, H_2O_2 as a superior product of sonication forms in solution (R6, R8, and R12), which is also a $\cdot\text{OH}$ radical scavenger (R13) [86]:



Protonation of superoxide ($\text{O}_2^{\cdot-}$) leads to the formation of uncharged $\text{HO}_2\cdot$ radicals in aqueous environments. These radicals have a $\text{p}K_a$ equal to 4.8. Therefore, it can be concluded that anion radicals are dominant in the physiological pH range. During the US process, hydrogen ($\text{H}\cdot$) radicals combine with molecular oxygen (O_2) and lead to the production of $\text{HO}_2\cdot$ radicals (R7). As mentioned above, the $\text{p}K_a$ value of $\text{HO}_2\cdot$ radicals equals 4.8. Therefore, when the pH exceeds 4.8, $\text{HO}_2\cdot$ radicals are not formed stably [53,87].

3.6. Synergistic effect

The synergistic effect was investigated to specify that the H_2O_2 oxidation process and the US method can intensify one another. In this regard, six laboratory tests (with two repetitions for each process) were performed. The studies' findings indicated that the H_2O_2 oxidation process and the US method can reinforce one another. A comparison of DBP removal (concentration of 10 mg/L) using different techniques, including US irradiation, H_2O_2 oxidation, and US/ H_2O_2 , is shown in Fig. 5. Degradation of DBP using only US leads to the kinetic constant of 0.0054 ($K = 0.0054$).

In contrast, using only H_2O_2 oxidation results in a kinetic constant of 0.105 ($K = 0.105$). Also, the US/ H_2O_2 process had a kinetic constant of 0.166 ($K = 0.166$) under the same experimental conditions. A synergistic effect was observed

in the US/ H_2O_2 process. So that the degradation rate of DBP in the US/ H_2O_2 process was higher than the sum degradation rate in each of the US and H_2O_2 processes. To show this synergistic effect, the following equation was used [53,87]:

$$S = \frac{K_{\text{US}} / \text{H}_2\text{O}_2}{K_{\text{US}} + K_{\text{H}_2\text{O}_2}} = \frac{0.166}{0.0054 + 0.105} = 1.5 \quad (13)$$

3.7. The H_2O_2 concentration variation

The changes in hydrogen peroxide production were evaluated to understand the reactions during the process. In this regard, one laboratory test was performed. Fig. S2 shows the changes in H_2O_2 production during 120 min. Based on the results, the concentration of H_2O_2 increased over time (1.5 to 7 mmol/L after 120 min). $\cdot\text{OH}$ and $\text{H}\cdot$ radicals are created by cavitation when an aqueous solution is exposed to US radiation. Because of its high oxidation potential, the $\cdot\text{OH}$ radical may directly oxidize organic substrates, leading to their mineralization or deterioration. Nevertheless, $\cdot\text{OH}$ radicals have a short half-life and quickly combine to produce H_2O_2 . There is a linear relationship between the H_2O_2 concentration produced and the US irradiation time [53,87]. A main by-product of US irradiation is H_2O_2 , which acts as an $\cdot\text{OH}$ scavenger and accumulates linearly in solution. Previous studies have proven that, during US irradiation at a constant intensity, the rate of production of $\cdot\text{OH}$ radicals can be assumed constant [53,87]. Therefore, the reaction of $\cdot\text{OH}$ radicals with each other and their conversion to H_2O_2 can be the reason for the increase in the concentration of H_2O_2 during the US irradiation time.

3.8. Real industrial wastewater treatment

To determine the removal efficiency of DBP by the US/ H_2O_2 system from real industrial wastewater, the wastewater samples (samples #1 and 2) were gathered from the

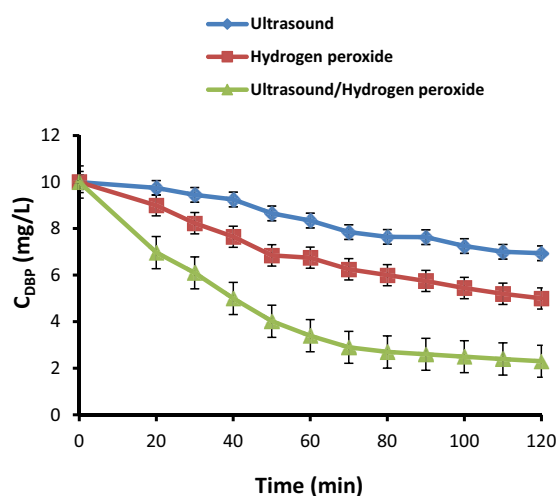


Fig. 5. Comparing the effectiveness of different treatment techniques for reducing DBP levels (type of wastewater: real, pH = 7, the concentration of H_2O_2 : 1.5 mmol/L, concentration of DBP: 10 mg/L, reaction time: 0–120 min, and frequency: 60 Hz).

input of two industrial wastewater treatment plants (IWTP). Following this, two laboratory tests (one test for each sample) were performed in optimal conditions. The physico-chemical properties of samples #1 and 2 are listed in Table S1. The collection of two samples from two different industrial treatment plants was because each treatment plant receives wastewater from various industries, such as the production of plastic containers, glue, polyethylene container, paint, cable, waterproofing, rubber, polymer, and cosmetic products. DBP was used as a raw material in these industries.

The Design–Expert software analysis (Fig. 6a) showed that the pH of 7, H_2O_2 concentration of 1.5 mmol/L, DBP concentration of 10 mg/L, and reaction time of 65 min were the optimal conditions (with 73% removal efficiency of DBP). The US/ H_2O_2 system treats the real and synthetic wastewater with efficiency close to that predicted by the Design–Expert. The DBP removal efficiency was approximately 70% in real wastewater (sample #1 = 66.85% and sample #2 = 74.22%) and 75.55% in synthetic wastewater (Fig. 6a). Ahmadi et al. [88] used H_2O_2 /MgO nanoparticles as AOPs to remove Reactive Blue 19 (RB19) dye from an aqueous solution. They applied RSM based on CCD for optimization of the AOPs. Researchers reported a removal efficiency of 93.77% under optimal conditions. In addition, the RB19 removal efficiency (%) achieved in the experiments was found to be quite similar to the anticipated response values. In Kyzas et al. [41] study, different AOPs such as ultrasonic/persulfate (US/PS), US/ H_2O_2 , US/ H_2O_2 /Fe²⁺, US/PS/Fe²⁺, and US/PS/ H_2O_2 /Fe²⁺ were evaluated and their potential in removing ciprofloxacin (CIP) was reported. The results showed, after 60 min, only 61.2% and 54.4% of the CIP was removed by US/PS and US/ H_2O_2 , respectively, but for US/PS/Fe²⁺ and US/ H_2O_2 /Fe²⁺ processes, the removal percentage has reached a significant amount of 86.6% and 72.2%, respectively. It can be related to the production of $SO_4^{\cdot -}$ and $\cdot OH$ and further activation of PS and H_2O_2 by divalent iron.

3.9. Mineralization of DBP

Mineralization tests were performed to determine whether mineralization (TOC removal) occurred during industrial wastewater treatment containing DBP with the US/ H_2O_2 system. In this regard, two laboratory tests (one test for each sample) were performed in optimal conditions. A TOC analyzer determined the TOC content of the samples at 800°C. Eq. (14) was used to calculate the TOC removal efficiency (%) [43,69]:

$$\text{TOC removal efficiency (\%)} = \frac{\text{TOC}_0 - \text{TOC}_t}{\text{TOC}_0} \times 100 \quad (14)$$

where TOC_0 is the concentration of TOC after adding DBP (10 mg/L) to wastewater (mg/L), and TOC_t is the concentration of TOC after the treatment of wastewater for 65 min (mg/L) (Table S1). Fig. 6b shows TOC removal efficiency in real industrial wastewater samples containing DBP by US/ H_2O_2 system. In sample #1, the DBP removal efficiency of 66.85% was achieved during 65 min, but the removal efficiency of TOC reached 56.5% after 65 min. In sample #2, DBP removal efficiency of 74.22% was achieved during 65 min, but TOC efficiency removal reached 58.92% after 65 min. These results showed that when DBP-containing industrial wastewater samples were treated with the US/ H_2O_2 system, significant mineralization occurred after 65 min. Al-Musawi et al. [42] investigated the removal of acid blue 80 dye by various AOPs (UV/ H_2O_2 , UV/PS, and UV/PS/ H_2O_2). The researchers reported that the amount of mineralization increases with increasing degradation time, and approximately 92.1% of the TOC is removed by using the combined system (UV/PS/ H_2O_2) in 120 min, whereas only 50.9% is removed by utilizing the UV/ H_2O_2 system and approximately 59.1% is removed by using the UV/PS system.

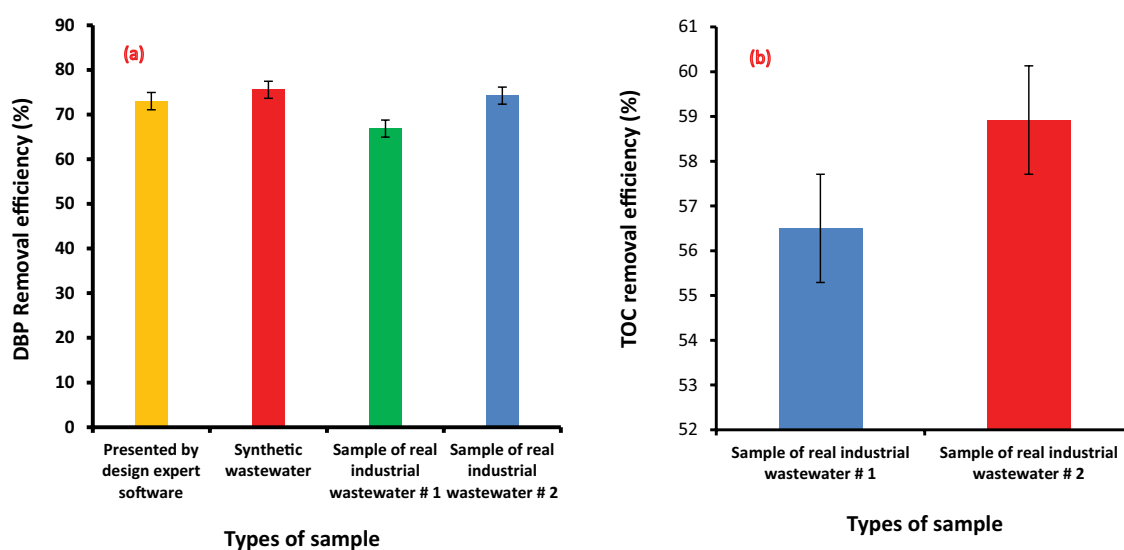


Fig. 6. (a) DBP removal efficiency proposed by Design–Expert software and DBP removal efficiency achieved by US/ H_2O_2 system in wastewater samples (real (samples #1 and 2) and synthetic) and (b) total organic carbon removal efficiency in real industrial wastewater samples containing DBP by US/ H_2O_2 system (type of wastewater: real, pH = 7, the concentration of H_2O_2 : 1.5 mmol/L, concentration of DBP: 10 mg/L, and reaction time: 65 min).

3.10. Formation of intermediate products during the degradation of DBP

Identification of intermediate products is essential in US/ H_2O_2 system. Because we find out whether toxic compounds are released from DBP decomposition into the aqueous solution. The GC-MS was used to investigate the intermediates produced during the removal of DBP by the US/ H_2O_2 system.

Following this purpose, one laboratory test was performed. The reactor containing synthetic wastewater was operated in the DBP concentration of 10 mg/L, pH = 7, H_2O_2 concentration of 1.5 mmol/L, reaction times of 15, 30, 60, 90 and 120 min, mixing speed of 700 rpm, and temperature of 25°C. Then, at the end of different reaction times, samples were taken from the effluent and analyzed by GC-MS. Based on the peaks obtained in the output chromatogram, a search was

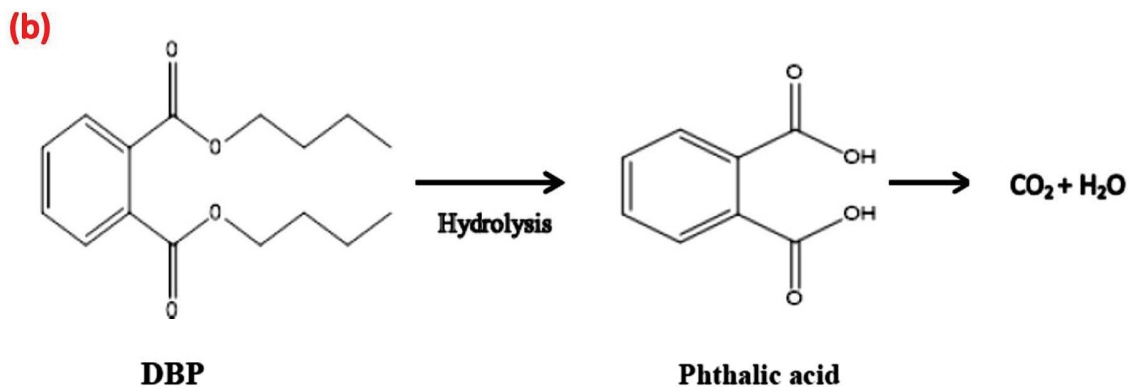
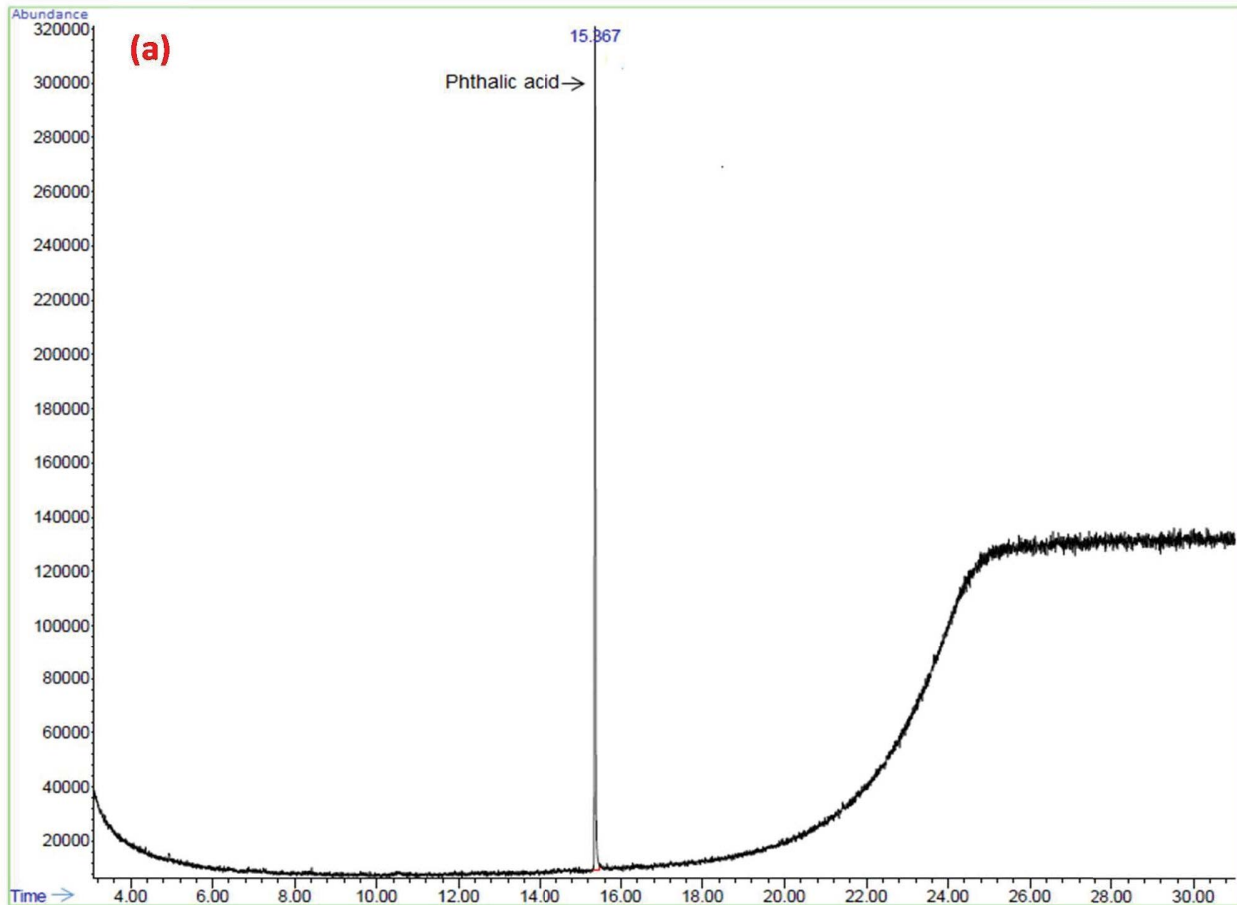


Fig. 7. (a) The GC-MS spectrum of intermediate products; (b) DBP to $C_8H_6O_4$ degradation pathway in the US/ H_2O_2 system (type of wastewater: synthetic, pH = 7, the concentration of H_2O_2 : 1.5 mmol/L, concentration of DBP: 10 mg/L, reaction time of 15, 30, 60, 90 and 120 min).

done in Wiley 2001 and the NIST library of GC-MS (identifying a probable compound with 90% specific confidence). Finally, the chemical structure and molecular weight of the possible compound were checked by Chem Draw Ultra software (version 12). Phthalic acid ($C_8H_6O_4$) as an intermediate product was identified. The GC-MS spectrum of intermediate products is shown in Fig. 7a.

Also, the degradation pathway of DBP to $C_8H_6O_4$ is illustrated in Fig. 7b. $C_8H_6O_4$ was derived from DBP hydrolysis

in the aliphatic chain. The aromatic ring of DBP remained intact. Hence, the aliphatic chain mainly initiated DBP degradation by the US/H_2O_2 system compared to the aromatic rings. Hydrolysis of DBP released ether groups into the aqueous medium. Ether groups can only act as hydrogen bond acceptors, making them have low solubility in water and evaporate quickly. Also, no significant toxicity to aquatic organisms is expected from the ether. The solubility of $C_8H_6O_4$ in water is high (5.74 g/L). There is evidence of the

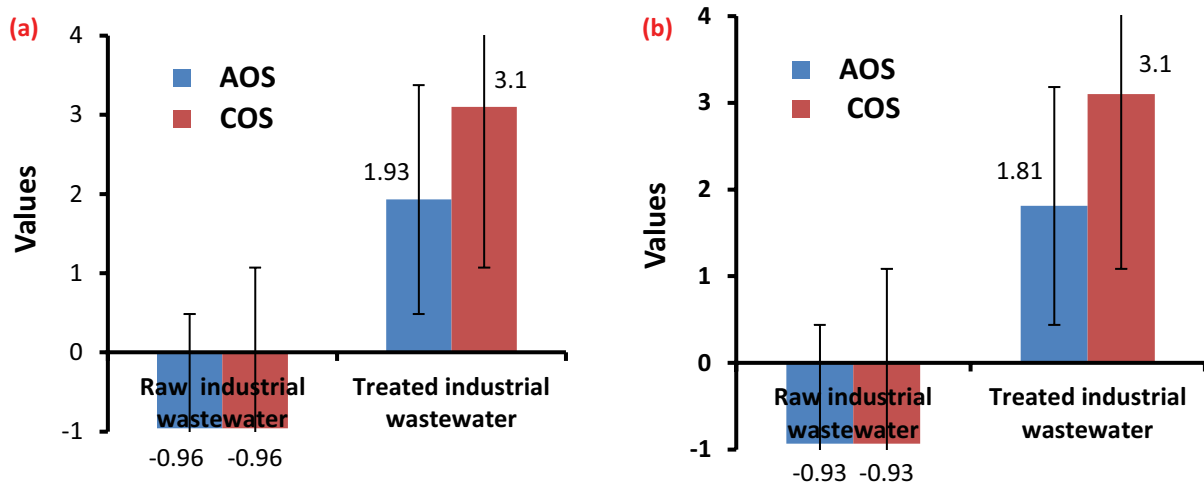


Fig. 8. AOS and COS values of samples # (a) 1 and (b) 2 in raw and treated wastewater (type of wastewater: real, pH = 7, the concentration of H_2O_2 : 1.5 mmol/L, concentration of DBP: 10 mg/L, and reaction time: 65 min).

Table 4

Values of parameters GP (%), GS, GI, and EC_{50} of wheat grains in treated wastewater sample (effluent) #1 in a period of 96 h (type of wastewater: real, pH = 7, concentration of H_2O_2 : 1.5 mmol/L, concentration of DBP: 10 mg/L, and reaction time: 65 min)

Process type	Time (h)	Effluent different dilutions and control sample	Parameters			
			GP (%)	GS	GI	EC_{50}
Removal process of DBP from wastewater sample #1 by the US/H_2O_2 system	24	1	0	0	0	9.51
		1/2	10	1.5	0.1	
		1/4	13.33	2	0.13	
		1/5	23.33	3.5	0.23	
		Distilled water	0	0	0	
	48	1	13.33	1	0.26	10.75
		1/2	56.66	4.25	1.13	
		1/4	63.33	4.75	1.26	
		1/5	66.66	5	1.33	
		Distilled water	40	3	0.8	
	72	1	20	1	0.6	10.75
		1/2	43.33	2.16	1.3	
		1/4	56.66	2.83	1.7	
		1/5	70	3.5	2.1	
		Distilled water	40	3	1.2	
	96	1	23.33	0.87	0.93	10.75
		1/2	46.66	1.75	1.86	
		1/4	60	2.25	2.4	
		1/5	73.33	2.75	2.93	
		Distilled water	40	1.5	1.6	

toxicity of $C_8H_6O_4$ in vitro and in vivo (developmental toxicity, reproductive toxicity, mutagenicity, etc.) [89]. Therefore, it can be concluded that in the decomposition of DBP by the US/ H_2O_2 system, producing $C_8H_6O_4$ as an intermediate is a severe problem.

3.11. Biodegradability studies

Biodegradability tests were performed to determine whether biodegradability improved when treating industrial wastewater containing DBP with the US/ H_2O_2 system. In this regard, two laboratory tests (one test for each sample) were performed in optimal conditions. We calculated the average oxidation state (AOS) and carbon oxidation state (COS) of wastewater for evaluating biodegradability enhancement. Eqs. (15) and (16) were used to calculate AOS and COS values [90]:

$$AOS = 4 - 1.5 \left(\frac{COD}{TOC} \right) \quad (15)$$

$$COS = 4 - 1.5 \left(\frac{COD}{TOC_0} \right) \quad (16)$$

where TOC is the TOC of the wastewater sample after treatment by the US/ H_2O_2 system, COD is the COD of the wastewater sample after treatment by the US/ H_2O_2 system, and TOC_0 is the concentration of TOC after adding DBP

(10 mg/L) to wastewater (mg/L) (Table S1). The values of AOS and COS range from –4 to +4.

In Fig. 8, values of AOS and COS for (a) sample #1 and (b) sample #2 are presented before and after treatment. For sample #1, the AOS value increased from –0.96 to 1.93, and the COS value increased from –0.96 to 3.1. Similarly, the AOS value for sample #2 increased from –0.93 to 1.81, and the COS value increased from –0.93 to 3.1. These results confirmed the relatively high degree of mineralization. Furthermore, these findings indirectly prove that the molecule of DBP was degraded into biodegradable by-products. Therefore, improving the biodegradability of real industrial wastewater was achieved using the US/ H_2O_2 system.

3.12. Biototoxicity analyses

An increase in the values of GP (%), GS, and GI parameters of wheat grains was observed with the increase in effluent dilution (Tables 4 and 5). Furthermore, this rise was more apparent for sample #2 than for sample #1. These findings imply that the US/ H_2O_2 system effectively reduced the toxicity of the industrial wastewater, and the toxicity of sample #2 was better eradicated. It was also discovered that when effluent dilution was enhanced, the toxicity of the effluent was reduced, and wheat seed germination increased (Tables 4 and 5).

EC_{50} in the output effluent sample #1 from US/ H_2O_2 system after 24, 48, 72, and 96 h was 9.51, 10.75, 10.75, and 10.75 mg/L, while in the effluent of sample #2 was 22.84, 62.95, 62.95, and 62.95 mg/L, respectively (Tables 4 and 5).

Table 5

Values of parameters GP (%), GS, GI, and EC_{50} of wheat grains in treated wastewater sample (effluent) #2 in a period of 96 h (type of wastewater: real, pH = 7, concentration of H_2O_2 : 1.5 mmol/L, concentration of DBP: 10 mg/L, and reaction time: 65 min)

Process type	Time (h)	Effluent different dilutions and control sample	Parameters			
			GP (%)	GS	GI	EC_{50}
Removal process of DBP from wastewater sample #2 by the US/ H_2O_2 system	24	1	10	1.5	0.1	22.84
		1/2	16.66	2.5	0.16	
		1/4	26.66	4	0.26	
		1/5	30	4.5	0.3	
		Distilled water	0	0	0	
	48	1	33.33	2.5	0.66	62.95
		1/2	60	4.5	1.2	
		1/4	63.33	4.75	1.26	
		1/5	83.33	6.25	1.66	
		Distilled water	40	3	0.8	
	72	1	36.66	1.83	1.1	62.95
		1/2	60	3	1.8	
		1/4	63.33	3.16	1.9	
		1/5	90	4.5	2.7	
		Distilled water	40	3	1.2	
	96	1	40	1.5	1.6	62.95
		1/2	63.33	2.37	2.53	
		1/4	66.66	2.5	2.66	
		1/5	90	3.37	3.6	
		Distilled water	40	3	1.6	

The EC_{50} value in effluents has increased from 24 h to 48 h. However, after that, the EC_{50} value was fixed. The lower EC_{50} in the first 24 h and sample #1 may be due to the higher number of wheat grains that have not rooted and germinated.

4. Conclusion

In this study, the performance of the US/ H_2O_2 system for the removal of DBP was evaluated, and this system was investigated in terms of mineralization, biotoxicity, reaction kinetics and thermodynamics, and biodegradability. The results showed that the pH of the solution, the concentration of H_2O_2 and DBP, and the reaction time had a significant influence on the performance of the US/ H_2O_2 system in the removal of DBP. In this regard, the efficiency of DBP removal was increased by enhancing reaction time. Nevertheless, the removal efficiency decreased as pH, DBP concentration, and H_2O_2 concentration increased. The US/ H_2O_2 system showed the capacity to degrade 70.53% of the DBP solution and minimized the toxicity of the effluent to wheat grains. The Design-Expert software analysis showed that the pH of 7, H_2O_2 concentration of 1.5 mmol/L, DBP concentration of 10 mg/L, and reaction time of 65 min were the optimal conditions (with 73% removal efficiency of DBP). Results of the kinetic models showed that the removal kinetics of DBP can be described by the first-order model ($R^2 = 0.99$). The negative values of ΔG° indicated that the chemical reaction using the US/ H_2O_2 system to degrade DBP spontaneously increased with temperature. A positive value of the ΔH° (0.3 kJ/mol) indicated that the oxidative reaction was endothermic. Also, a positive value of the ΔS° (1.054 J/mol·K), showed that the transition state was highly disordered relative to the ground state. The study findings showed a relatively high degree of mineralization. As US/ H_2O_2 system converted nonbiodegradable wastewater into biodegradable effluent, it was proposed that this system be used as a pretreatment process before the biological treatment of industrial wastewater prior to discharge into the ecological system. $C_8H_6O_4$ was produced as a toxic intermediate compound in the decomposition process of DBP by the US/ H_2O_2 system, which should be given serious attention. Toxicity tests showed that the effluent generated by the US/ H_2O_2 system had low toxicity, so wheat seeds sprouted satisfactorily after 96 h. A concentration of DBP at which 50% of wheat grains do not germinate, so-called LC_{50} , was determined as 10.75 and 62.95 mg/L after 96 h for effluent samples #1 and 2, respectively.

We concluded that US/ H_2O_2 is a relatively effective process with non-toxic production effluent. However, to decide whether this process is economical compared to other processes, the removal of DBP by other processes should be tested, and an economic evaluation should be done. Finally, it is possible to decide which process is more economical based on quantitative results. Furthermore, it is suggested to perform more toxicity evaluation tests based on the environmental standards for discharging the process effluent into the environment.

Acknowledgements

This research was part of a PhD thesis entitled “Application of Ultrasound/hydrogen peroxide system for

DBP removal with a focus on optimization by a response surface method: Effective factors, pathway and biodegradability studies” with the ethics approval code of IR.KMU.REC.1400.122 and Reg. No.400000078, conducted at the Environmental Health Engineering Research Center and sponsored by the Vice-Chancellor for Research and Technology of Kerman University of Medical Sciences. The authors express their gratitude for the support and assistance extended by the facilitators during the research process.

Declaration of competing interest

The authors declare that they have no known competing financial interests or personal relationships that could have appeared to influence the work reported in this paper.

References

- [1] H. Ye, B. Zhao, Y. Zhou, J. Du, M. Huang, Recent advances in adsorbents for the removal of phthalate esters from water: material, modification, and application, *Chem. Eng. J.*, 409 (2021) 128127, doi: 10.1016/j.cej.2020.128127.
- [2] H. Amiri, S.S. Martinez, M.A. Shiri, M.M. Soori, Advanced oxidation processes for phthalate esters removal in aqueous solution: a systematic review, *Rev. Environ. Health*, 37 (2022) 1–22.
- [3] M. Gao, Y. Zhang, X. Gong, Z. Song, Z. Guo, Removal mechanism of di-*n*-butyl phthalate and oxytetracycline from aqueous solutions by nano-manganese dioxide modified biochar, *Environ. Sci. Pollut. Res.*, 25 (2018) 7796–7807.
- [4] M. Bodzek, M. Dudziak, K. Luks-Betlej, Application of membrane techniques to water purification. Removal of phthalates, *Desalination*, 162 (2004) 121–128.
- [5] M.A. Shaida, R. Dutta, A. Sen, Removal of diethyl phthalate via adsorption on mineral rich waste coal modified with chitosan, *J. Mol. Liq.*, 261 (2018) 271–282.
- [6] S.V. Mohan, S. Shailaja, M.R. Krishna, P. Sarma, Adsorptive removal of phthalate ester (di-ethyl phthalate) from aqueous phase by activated carbon: a kinetic study, *J. Hazard. Mater.*, 146 (2007) 278–282.
- [7] I. Al-Saleh, R. Elkhatib, T. Al-Rajoudi, G. Al-Qudaihi, Assessing the concentration of phthalate esters (PAEs) and bisphenol A (BPA) and the genotoxic potential of treated wastewater (final effluent) in Saudi Arabia, *Sci. Total Environ.*, 578 (2017) 440–451.
- [8] T. Wang, T. Liu, Pulse electro-coagulation application in treating dibutyl phthalate wastewater, *Water Sci. Technol.*, 76 (2017) 1124–1131.
- [9] H.-T. Gao, R. Xu, W.-X. Cao, L.-L. Qian, M. Wang, L.-G. Lu, Q. Xu, S.-Q. Yu, Effects of six priority controlled phthalate esters with long-term low-dose integrated exposure on male reproductive toxicity in rats, *Food Chem. Toxicol.*, 101 (2017) 94–104.
- [10] S. Harris, S.A. Hermsen, X. Yu, S.W. Hong, E.M. Faustman, Comparison of toxicogenomic responses to phthalate ester exposure in an organotypic testis co-culture model and responses observed in vivo, *Reprod. Toxicol.*, 58 (2015) 149–159.
- [11] M. Mariana, J. Feiteiro, I. Verde, E. Cairrao, The effects of phthalates in the cardiovascular and reproductive systems: a review, *Environ. Int.*, 94 (2016) 758–776.
- [12] H.-T. Gao, R. Xu, W.-X. Cao, Q.-N. Di, R.-X. Li, L.-G. Lu, Q. Xu, S.-Q. Yu, Combined effects of simultaneous exposure to six phthalates and emulsifier glycerol monostearate on male reproductive system in rats, *Toxicol. Appl. Pharmacol.*, 341 (2018) 87–97.
- [13] R. Benson, Hazard to the developing male reproductive system from cumulative exposure to phthalate esters—dibutyl phthalate, diisobutyl phthalate, butylbenzyl phthalate, diethylhexyl phthalate, dipentyl phthalate, and diisononyl phthalate, *Regul. Toxicol. Pharm.*, 53 (2009) 90–101.

- [14] J. Yang, R. Hauser, R.H. Goldman, Taiwan food scandal: the illegal use of phthalates as a clouding agent and their contribution to maternal exposure, *Food Chem. Toxicol.*, 58 (2013) 362–368.
- [15] Y. Kang, Y.B. Man, K.C. Cheung, M.H. Wong, Risk assessment of human exposure to bioaccessible phthalate esters via indoor dust around the Pearl River Delta, *Environ. Sci. Technol.*, 46 (2012) 8422–8430.
- [16] A. Musolf, S. Leschik, M. Möder, G. Strauch, F. Reinstorf, M. Schirmer, Temporal and spatial patterns of micropollutants in urban receiving waters, *Environ. Pollut.*, 157 (2009) 3069–3077.
- [17] K. Khosravi, G.W. Price, Determination of phthalates in soils and biosolids using accelerated solvent extraction coupled with SPE cleanup and GC-MS quantification, *Microchem. J.*, 121 (2015) 205–212.
- [18] A. Saini, J.O. Okeme, E. Goosey, M.L. Diamond, Calibration of two passive air samplers for monitoring phthalates and brominated flame-retardants in indoor air, *Chemosphere*, 137 (2015) 166–173.
- [19] A. Alkenani, T.A. Saleh, Synthesis of amine-modified graphene integrated membrane as protocols for simultaneous rejection of hydrocarbons pollutants, metal ions, and salts from water, *J. Mol. Liq.*, 367 (2022) 120291, doi: 10.1016/j.molliq.2022.120291.
- [20] T.A. Saleh, Protocols for synthesis of nanomaterials, polymers, and green materials as adsorbents for water treatment technologies, *Environ. Technol. Innovation*, 24 (2021) 101821, doi: 10.1016/j.eti.2021.101821.
- [21] T.A. Saleh, Nanomaterials: classification, properties, and environmental toxicities, *Environ. Technol. Innovation*, 20 (2020) 101067, doi: 10.1016/j.eti.2020.101067.
- [22] T.A. Saleh, A. Sari, M. Tuzen, Simultaneous removal of polyaromatic hydrocarbons from water using polymer modified carbon, *Biomass Convers. Biorefin.*, (2022) 1–10, doi: 10.1007/s13399-021-02163-9.
- [23] T.A. Saleh, M. Mustaqeem, M. Khaled, Water treatment technologies in removing heavy metal ions from wastewater: a review, *Environ. Nanotechnol. Monit. Manage.*, 17 (2022) 100617, doi: 10.1016/j.enmm.2021.100617.
- [24] T.A. Saleh, A.M. Musa, S.A. Ali, Synthesis of hydrophobic cross-linked polyzwitterionic acid for simultaneous sorption of Eriochrome black T and chromium ions from binary hazardous waters, *J. Colloid Interface Sci.*, 468 (2016) 324–333.
- [25] S.A. Ali, I.B. Rachman, T.A. Saleh, Simultaneous trapping of Cr(III) and organic dyes by a pH-responsive resin containing zwitterionic aminomethylphosphonate ligands and hydrophobic pendants, *Chem. Eng. J.*, 330 (2017) 663–674.
- [26] T.A. Saleh, A.M. Elsharif, O.A. Bin-Dahman, Synthesis of amine functionalization carbon nanotube-low symmetry porphyrin derivatives conjugates toward dye and metal ions removal, *J. Mol. Liq.*, 340 (2021) 117024, doi: 10.1016/j.molliq.2021.117024.
- [27] A.M. Osman, A.H. Hendi, T.A. Saleh, Simultaneous adsorption of dye and toxic metal ions using an interfacially polymerized silica/polyamide nanocomposite: kinetic and thermodynamic studies, *J. Mol. Liq.*, 314 (2020) 113640, doi: 10.1016/j.molliq.2020.113640.
- [28] T.A. Saleh, G. Fadillah, E. Ciptawati, M. Khaled, Analytical methods for mercury speciation, detection, and measurement in water, oil, and gas, *TrAC, Trends Anal. Chem.*, 132 (2020) 116016, doi: 10.1016/j.trac.2020.116016.
- [29] A.A. Alazab, T.A. Saleh, Magnetic hydrophobic cellulose-modified polyurethane filter for efficient oil-water separation in a complex water environment, *J. Water Process Eng.*, 50 (2022) 103125, doi: 10.1016/j.jwpe.2022.103125.
- [30] T.A. Saleh, Carbon nanotube-incorporated alumina as a support for MoNi catalysts for the efficient hydrodesulfurization of thiophenes, *Chem. Eng. J.*, 404 (2021) 126987, doi: 10.1016/j.cej.2020.126987.
- [31] O.A. Bin-Dahman, T.A. Saleh, Synthesis of polyamide grafted on biosupport as polymeric adsorbents for the removal of dye and metal ions, *Biomass Convers. Biorefin.*, (2022) 1–14, doi: 10.1007/s13399-022-02382-8.
- [32] G. Fadillah, T.A. Saleh, S. Wahyuningsih, Enhanced electrochemical degradation of 4-Nitrophenol molecules using novel Ti/TiO₂-NiO electrodes, *J. Mol. Liq.*, 289 (2019) 111108, doi: 10.1016/j.molliq.2019.111108.
- [33] T.A. Saleh, Characterization, determination and elimination technologies for sulfur from petroleum: toward cleaner fuel and a safe environment, *Trends Environ. Anal. Chem.*, 25 (2020) e00080, doi: 10.1016/j.teac.2020.e00080.
- [34] D. Jin, X. Kong, Y. Li, Z. Bai, G. Zhuang, X. Zhuang, Y. Deng, Biodegradation of di-*n*-butyl phthalate by *Achromobacter* sp. isolated from rural domestic wastewater, *Int. J. Environ. Res. Public Health*, 12 (2015) 13510–13522.
- [35] C. Chan, K. Wong, W. Chung, T. Chow, P. Wong, Photocatalytic degradation of di(2-ethylhexyl)phthalate adsorbed by chitin A, *Water Sci. Technol.*, 56 (2007) 125–134.
- [36] S. Ziembowicz, M. Kida, P. Koszelnik, Removal of dibutyl phthalate (DBP) from landfill leachate using an ultrasonic field, *Desal. Water Treat.*, 117 (2018) 9–14.
- [37] Y. Yang, Z.W. Lin, Study on the degradation of plasticizer di(2-ethylhexyl)phthalate by advanced oxidation process, *Adv. Mater. Res.*, 529 (2012) 463–467.
- [38] L. Wang, G.Y. Fu, B. Zhao, Z. Zhang, X. Guo, H. Zhang, Degradation of di-*n*-butyl phthalate in aqueous solution by the O₃/UV process, *Desal. Water Treat.*, 52 (2014) 824–833.
- [39] N.A. Medellin Castillo, R. Ocampo Perez, R. Leyva Ramos, M. Sanchez Polo, J. Rivera Utrilla, J.D. Méndez Diaz, Removal of diethyl phthalate from water solution by adsorption, photo-oxidation, ozonation and advanced oxidation process (UV/H₂O₂, O₃/H₂O₂ and O₃/activated carbon), *Sci. Total Environ.*, 442 (2013) 26–35.
- [40] L. Mansouri, C. Tizaoui, S.-U. Geissen, L. Bousseml, A comparative study on ozone, hydrogen peroxide and UV based advanced oxidation processes for efficient removal of diethyl phthalate in water, *J. Hazard. Mater.*, 363 (2019) 401–411.
- [41] G.Z. Kyzas, N. Mengelizadeh, M. khodadadi Saloot, S. Mohebi, D. Balarak, Sonochemical degradation of ciprofloxacin by hydrogen peroxide and persulfate activated by ultrasound and ferrous ions, *Colloids Surf., A*, 642 (2022) 128627, doi: 10.1016/j.colsurfa.2022.128627.
- [42] T.J. Al-Musawi, M. Yilmaz, S. Mohebi, D. Balarak, Ultraviolet radiation/persulfate/hydrogen peroxide treatment system for the degradation of acid blue 80 dye from a batch flow chemical reactor: effects of operational parameters, mineralization, energy consumption, and kinetic studies, *Energy Ecol. Environ.*, 7 (2022) 630–640.
- [43] K.H. Chu, Y.A. Al-Hamadani, C.M. Park, G. Lee, M. Jang, A. Jang, N. Her, A. Son, Y.M. Yoon, Ultrasonic treatment of endocrine disrupting compounds, pharmaceuticals, and personal care products in water: a review, *Chem. Eng. J.*, 327 (2017) 629–647.
- [44] Y. Yoon, Y. Hwang, M. Kwon, Y. Jung, T.-M. Hwang, J.-W. Kang, Application of O₃ and O₃/H₂O₂ as post-treatment processes for color removal in swine wastewater from a membrane filtration system, *J. Ind. Eng. Chem.*, 20 (2014) 2801–2805.
- [45] Z. Shu, J.R. Bolton, M. Belosevic, M.G. El Din, Photodegradation of emerging micropollutants using the medium-pressure UV/H₂O₂ advanced oxidation process, *Water Res.*, 47 (2013) 2881–2889.
- [46] J.G. Lin, C.N. Chang, J.R. Wu, Decomposition of 2-chlorophenol in aqueous solution by ultrasound/H₂O₂ process, *Water Sci. Technol.*, 33 (1996) 75–81.
- [47] S. Rahdar, C.A. Igwegbe, M. Ghasemi, S. Ahmadi, Degradation of aniline by the combined process of ultrasound and hydrogen peroxide (US/H₂O₂), *MethodsX*, 6 (2019) 492–499.
- [48] A. Seid-Mohammadi, G. Asgarai, Z. Ghorbanian, A. Dargahi, The removal of cephalixin antibiotic in aqueous solutions by ultrasonic waves/hydrogen peroxide/nickel oxide nanoparticles (US/H₂O₂/NiO) hybrid process, *Sep. Sci. Technol.*, 55 (2020) 1558–1568.
- [49] M. Dehghani, Y. Kamali, F. Jamshidi, M.A. Shiri, M. Nozari, Contribution of H₂O₂ in ultrasonic systems for degradation of DR-81 dye from aqueous solutions, *Desal. Water Treat.*, 107 (2018) 332–339.

- [50] APHA, Standard Methods for the Examination of Water and Wastewater, In "4500-S2- SULFIDE", Standard Methods for the Examination of Water and Wastewater, APHA-AWWA-WEF, Washington, D.C., USA, 2018.
- [51] M. Moazzen, A.H. Mahvi, N. Shariatifar, G. Jahed Khaniki, S. Nazmara, M. Alimohammadi, R. Ahmadkhaniha, N. Rastkari, M. Ahmadloo, A. Akbarzadeh, S. Dobaradaran, A.N. Baghani, Determination of phthalate acid esters (PAEs) in carbonated soft drinks with MSPE/GC-MS method, *Toxin Rev.*, 37 (2018) 319–326.
- [52] S. Net, A. Delmont, R. Sempéré, A. Paluselli, B. Ouddane, Reliable quantification of phthalates in environmental matrices (air, water, sludge, sediment and soil): a review, *Sci. Total Environ.*, 515–516 (2015) 162–180.
- [53] Y. Nosaka, A.Y. Nosaka, Generation and detection of reactive oxygen species in photocatalysis, *Chem. Rev.*, 117 (2017) 11302–11336.
- [54] Y. Cai, Y.e. Cai, Y. Shi, J. Liu, S. Mou, Y. Lu, A liquid–liquid extraction technique for phthalate esters with water-soluble organic solvents by adding inorganic salts, *Microchim. Acta*, 157 (2007) 73–79.
- [55] M. Nozari, M. Malakootian, N. Jafarzadeh Haghighi Fard, H. Mahmoudi-Moghaddam, Synthesis of $Fe_3O_4@PAC$ as a magnetic nano-composite for adsorption of dibutyl phthalate from the aqueous medium: modeling, analysis and optimization using the response surface methodology, *Surf. Interfaces*, 31 (2022) 101981, doi: 10.1016/j.surfin.2022.101981.
- [56] M.H. Dehghani, A.H. Mahvi, N. Rastkari, R. Saeedi, S. Nazmara, E. Irvani, Adsorption of bisphenol A (BPA) from aqueous solutions by carbon nanotubes: kinetic and equilibrium studies, *Desal. Water Treat.*, 54 (2015) 84–92.
- [57] H. Li, P. Wang, W. Liu, Removal of dibutyl phthalate (DBP) from aqueous solution by adsorption using vanillin-modified chitosan beads (CTSV), *Desal. Water Treat.*, 56 (2015) 452–462.
- [58] M. Matouq, Z. Al-Anber, N. Susumu, T. Tagawa, H. Karapanagioti, The kinetic of dyes degradation resulted from food industry in wastewater using high frequency of ultrasound, *Sep. Purif. Technol.*, 135 (2014) 42–47.
- [59] J. Khan, M. Tariq, M. Muhammad, M.H. Mehmood, I. Ullah, A. Raziq, F. Akbar, M. Saqib, A. Rahim, A. Niaz, Kinetic and thermodynamic study of oxidative degradation of acid yellow 17 dye by Fenton-like process: effect of HCO_3^- , CO_3^{2-} , Cl^- and SO_4^{2-} on dye degradation, *Bull. Chem. Soc. Ethiop.*, 33 (2019) 243–254.
- [60] V.A. Jideani, S.M. Mpotokwana, Modeling of water absorption of Botswana bambara varieties using Peleg's equation, *J. Food Eng.*, 92 (2009) 182–188.
- [61] V.A. Jideani, I. Nkama, E.B. Agbo, I.A. Jideani, Mathematical modeling of odor deterioration of millet (*Pennisetum glaucum*) dough (*fura*) as affected by time-temperature and product packaging parameters, *Cereal Chem.*, 79 (2002) 710–714.
- [62] L. Sanchez, J.M. Peiro, H. Castillo, M.D. Perez, J.M. Ena, M. Calvo, Kinetic parameters for denaturation of bovine milk lactoferrin, *J. Food Sci.*, 57 (1992) 873–879.
- [63] F.D. Montanuci, L.M. de M. Jorge, R.M.M. Jorge, Kinetic, thermodynamic properties, and optimization of barley hydration, *Food Sci. Technol.*, 3 (2013) 690–698.
- [64] F. Gholami Borujeni, A. Zahedi, M. Sheikhi, Evaluation of hospital treated wastewater on seed germination and plant growth indices, *J. Health Res. Community*, 5 (2019) 49–59.
- [65] R.I. Khaleel, N. Ismail, M.H. Ibrahim, The impact of wastewater treatments on seed germination and biochemical parameter of *Abelmoschus esculentus* L., *Procedia - Soc. Behav. Sci.*, 91 (2013) 453–460.
- [66] M. Gao, Y. Qi, W. Song, H. Xu, Effects of di-*n*-butyl phthalate and di(2-ethylhexyl)phthalate on the growth, photosynthesis, and chlorophyll fluorescence of wheat seedlings, *Chemosphere*, 151 (2016) 76–83.
- [67] T.A. Saleh, M. Tuzen, A. Sari, Effective antimony removal from wastewaters using polymer modified sepiolite: isotherm kinetic and thermodynamic analysis, *Chem. Eng. Res. Des.*, 184 (2022) 215–223.
- [68] A. Sari, T.A. Saleh, M. Tuzen, Development and characterization of polymer-modified vermiculite composite as novel highly-efficient adsorbent for water treatment, *Surf. Interfaces*, 27 (2021) 101504, doi: 10.1016/j.surfin.2021.101504.
- [69] M.H. Dehghani, R.R. Karri, Z.T. Yeganeh, A.H. Mahvi, H. Nourmoradi, M. Salari, A. Zarei, M. Sillanpää, Statistical modelling of endocrine disrupting compounds adsorption onto activated carbon prepared from wood using CCD-RSM and DE hybrid evolutionary optimization framework: comparison of linear vs non-linear isotherm and kinetic parameters, *J. Mol. Liq.*, 302 (2020) 112526, doi: 10.1016/j.molliq.2020.112526.
- [70] S. Ziembowicz, M. Kida, P. Koszelnik, Sonochemical formation of hydrogen peroxide, *Proceedings*, 2 (2017) 188, doi: 10.3390/ecws-2-04957.
- [71] Y. Jiang, C. Pétrier, T.D. Waite, Effect of pH on the ultrasonic degradation of ionic aromatic compounds in aqueous solution, *Ultrason. Sonochem.*, 9 (2002) 163–168.
- [72] C. Pétrier, The Use of Power Ultrasound for Water Treatment, J.A. Gallego-Juarez, K.F. Graff, Eds., *Power Ultrasonics*, Elsevier, France, 2015, pp. 939–972.
- [73] L. Xu, W. Chu, N. Graham, A systematic study of the degradation of dimethyl phthalate using a high-frequency ultrasonic process, *Ultrason. Sonochem.*, 20 (2013) 892–899.
- [74] E. Villaroel, J. Silva-Agredo, C. Petrier, G. Taborda, R.A. Torres-Palma, Ultrasonic degradation of acetaminophen in water: effect of sonochemical parameters and water matrix, *Ultrason. Sonochem.*, 21 (2014) 1763–1769.
- [75] M. Lim, Y. Son, J. Khim, The effects of hydrogen peroxide on the sonochemical degradation of phenol and bisphenol A, *Ultrason. Sonochem.*, 21 (2014) 1976–1981.
- [76] Y. Ku, Y.H. Tu, C.M. Ma, Effect of hydrogen peroxide on the decomposition of monochlorophenols by sonolysis in aqueous solution, *Water Res.*, 39 (2005) 1093–1098.
- [77] S. Nélieu, L. Kerhoas, J. Einhorn, Degradation of atrazine into ammeline by combined ozone/hydrogen peroxide treatment in water, *Environ. Sci. Technol.*, 34 (2000) 430–437.
- [78] S. Esplugas, J. Gimenez, S. Contreras, E. Pascual, M. Rodríguez, Comparison of different advanced oxidation processes for phenol degradation, *Water Res.*, 36 (2002) 1034–1042.
- [79] I. Iordache, M. Nechita, N. Aelenei, I. Rosca, G. Apostolescu, M. Peptanariu, Sonochemical enhancement of cyanide ion degradation from wastewater in the presence of hydrogen peroxide, *Pol. J. Environ. Stud.*, 12 (2003) 735–738.
- [80] S. Na, C. Jinhua, M. Cui, J. Khim, Sonophotolytic diethyl phthalate (DEP) degradation with UVC or VUV irradiation, *Ultrason. Sonochem.*, 19 (2012) 1094–1098.
- [81] I. Hua, U. Pfalzer Thompson, Ultrasonic irradiation of carbofuran: decomposition kinetics and reactor characterization, *Water Res.*, 35 (2001) 1445–1452.
- [82] L.K. Weavers, N. Malmstadt, M.R. Hoffmann, Kinetics and mechanism of pentachlorophenol degradation by sonication, ozonation, and sonolytic ozonation, *Environ. Sci. Technol.*, 34 (2000) 1280–1285.
- [83] C.A. Igwegbe, S. Ahmadi, S. Rahdar, A. Ramazani, A.R. Mollazehi, Efficiency comparison of advanced oxidation processes for ciprofloxacin removal from aqueous solutions: sonochemical, sono-nano-chemical and sono-nano-chemical/persulfate processes, *Environ. Eng. Res.*, 25 (2020) 178–185.
- [84] M. Yegane Badi, M. Vosoughi, H. Sadeghi, S.A. Mokhtari, J. Mehralipour, Ultrasonic-assisted H_2O_2/TiO_2 process in catechol degradation: kinetic, synergistic and optimisation via response surface methodology, *Int. J. Environ. Anal. Chem.*, 102 (2022) 757–770.
- [85] A.-R.A. Giwa, I.A. Bello, A.B. Olabintan, O.S. Bello, T.A. Saleh, Kinetic and thermodynamic studies of Fenton oxidative decolorization of methylene blue, *Heliyon*, 6 (2020) e04454, doi: 10.1016/j.heliyon.2020.e04454.
- [86] G.V. Buxton, C.L. Greenstock, W.P. Helman, A.B. Ross, Critical review of rate constants for reactions of hydrated electrons, hydrogen atoms and hydroxyl radicals ($^{\bullet}OH/^{\bullet}O$ in aqueous solution), *J. Phys. Chem. Ref. Data*, 17 (1988) 513–886.

- [87] X. Li, J. Yu, M. Jaroniec, Hierarchical photocatalysts, *Chem. Soc. Rev.*, 45 (2016) 2603–2636.
- [88] S. Ahmadi, L. Mohammadi, C.A. Igwegbe, S. Rahdar, A.M. Banach, Application of response surface methodology in the degradation of Reactive Blue 19 using H_2O_2/MgO nanoparticles advanced oxidation process, *Int. J. Ind. Chem.*, 9 (2018) 241–253.
- [89] I.K. Lee, B.M. Lee, Toxicological characterization of phthalic acid, *Toxicol. Res.*, 27 (2011) 191–203.
- [90] N. Jaafarzadeh, A. Takdastan, S. Jorfi, F. Ghanbari, M. Ahmadi, G. Barzegar, The performance study on ultrasonic/ Fe_3O_4/H_2O_2 for degradation of azo dye and real textile wastewater treatment, *J. Mol. Liq.*, 256 (2018) 462–470.

$$\ln(C_t) = K_1 t + \ln(C_0) \quad (S1)$$

$$\text{Half-life (min)} = \frac{\ln 2}{K_1} \quad (S2)$$

where K_1 is the first-order degradation rate constant (min^{-1}) and can be calculated from $\ln(C_t)$ slope vs. t . C_0 is the initial concentration of dibutyl phthalate (DBP) in the solution (mg/L) as well as C_t is the DBP concentration in the solution (mg/L) at any time.

Supporting information

S1. Degradation kinetics

The first-order kinetics linear model and its half-life equation were as follows:

Table S1

Physico-chemical characteristics (TOC, BOD_5 , COD, TDS, TSS, nitrate, phosphate, sulfate, pH, and DBP concentration) of industrial wastewater samples (raw, after adding DBP with a concentration of 10 mg/L, and treated)

Parameters	Amounts related to sample #1	BOD_5 , COD, and TOC related to sample #1 after adding DBP (10 mg/L)	TOC and COD related to sample #1 after treatment	Amounts related to sample #2	BOD_5 , COD, and TOC related to sample #2 after adding DBP (10 mg/L)	TOC and COD related to sample #2 after treatment
TOC	16.1 (mg/L)	200 (mg/L)	87 (mg/L)	99 (mg/L)	224 (mg/L)	92 (mg/L)
BOD_5	8 (mg/L)	246 (mg/L)	–	40 (mg/L)	275 (mg/L)	–
COD	20 (mg/L)	350 (mg/L)	120 (mg/L)	101.7 (mg/L)	400 (mg/L)	134 (mg/L)
TDS	969 (mg/L)	–	–	7,322 (mg/L)	–	–
TSS	2.5 (mg/L)	–	–	256 (mg/L)	–	–
Nitrate	13.5 (mg/L)	–	–	N.D* (mg/L)	–	–
Phosphate	135 (mg/L)	–	–	4.76 (mg/L)	–	–
Sulfate	15.5 (mg/L)	–	–	13 (mg/L)	–	–
pH	7.68	–	–	6.89	–	–
DBP	10 (mg/L)	–	–	10 (mg/L)	–	–

*N.D: No detectable

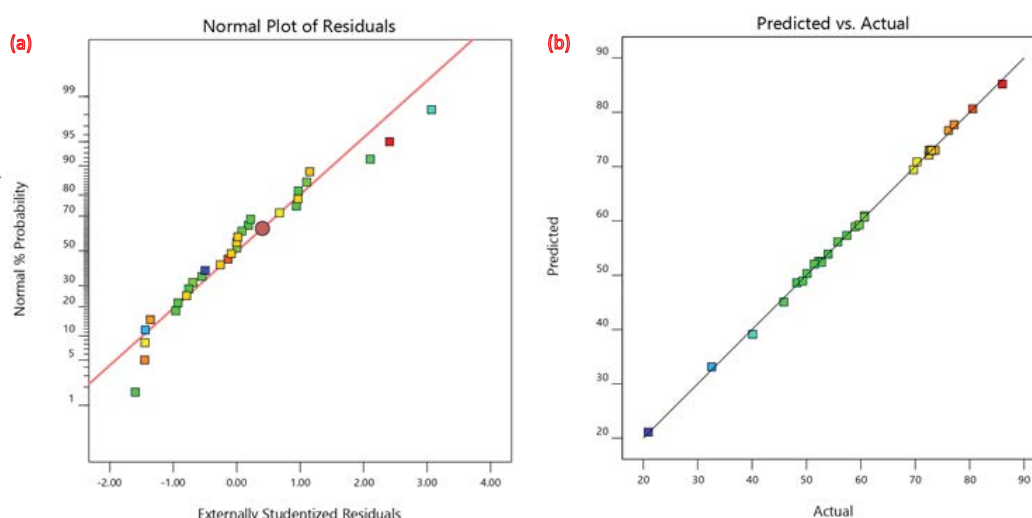


Fig. S1. (a) Normal probability plot of the residuals and (b) predicted vs. actual values plot for removal efficiency.

the total suspended solids (TSS), the total dissolved solids (TDS), nitrate, phosphate, sulfate, and DBP in the sample #1 were 16.1, 20, 8, 2.5, 969, 13.5, 135, 15.5 and 10, respectively. The concentrations (mg/L) of TOC, COD, BOD₅, TSS, TDS, phosphate, sulfate, and DBP in the sample #2 were 99, 101.7, 40, 256, 7,322, 4.76, 13 and 10, respectively. The pH of samples #1 and 2 were 7.68 and 6.89, respectively (Table S1).

S2.1. Suitable model, equations, and analysis of variance analysis

Fig. S1a indicates the normal probability plot of the residuals. Fig. S1b shows the actual vs. predicted values graph for removal efficiency.

S3. The H₂O₂ concentration variation

Fig. S2 shows the changes in H₂O₂ production during 120 min. Based on the results, the concentration of H₂O₂ increased over time (1.5 to 7 mmol/L after 120 min).

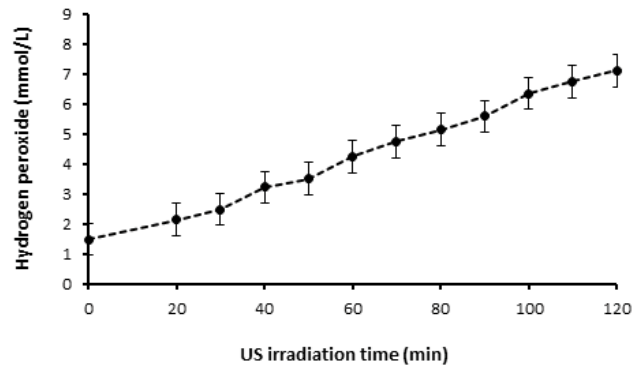


Fig. S2. The H₂O₂ concentration variation during the US irradiation time (H₂O₂ concentration of 1.5 mmol/L, pH = 7, DBP concentration of 10 mg/L, the reaction time of 120 min, mixing speed of 700 rpm and temperature of 25°C).